Universität für Bodenkultur Wien
University of Natural Resources and Life Sciences, Vienna
Department of Water, Atmosphere and Environment
Institute for Soil Physics and Rural Water Management

FROM GREY TO GREEN CITIES

INVESTIGATING THE INORGANIC NITROGEN AND THE WATER-HEAT FLUXES IN BIOROOFS

SUBMITTED BY

IOANNIS ARISTOTELIS PAPAGRIGORIOU

11831393

MASTER THESIS

In partial fulfilment of the requirements for the degree of

"DIPLOM-INGENIEUR"

Supervisor: Christine Stumpp, Univ.-Prof.Dr.

Co-supervisors: Efstathios Diamantopoulos, Ass.Prof.Dr.

Giuseppe Brunetti, Dr.

Acknowledgements

I would like to express my deep gratitude to Professor Christine Stumpp and Professor Eftsathios Diamantopoulos, my research supervisors, for their guidance and useful critiques of this research work. I would also like to thank Dr. Giuseppe Brunetti, whose guidance and suggestions made a significant contribution to the planning and development of the experiment, as well as his support with Python.

My grateful thanks are also extended to Mr. Wolfgang Sokol for setting up the acquisition system and Mrs. Martina Faulhammer as well as the rest of the laboratory technitians for their assistance during the laboratory analyses. Furthermore, I would like to thank my friend Wiebke Mareile Heinze for her help with the translation of the Abstract into German. Finally, I cannot forget to thank my family, my friends and my partner for the unconditional support during my Master Degree.

Abstract

By 2050, 70% of the world population will live in cities. Green Infrastructure is a fundamental tool to sustainable urban development. Considering that rooftops represent up to 50% of impervious surfaces in urban areas, they provide a great opportunity to integrate natural solutions and provide multiple ecosystem services. In this view, the novel technology that combines Green Roofs and Constructed Wetlands is represented by BioRoofs. BioRoofs are able to provide low-cost decentralised wastewater treatment, while moderating high temperatures in cities and reducing water surface runoff in building and urban scale. So far, a few studies have investigated the water quality performance of BioRoofs with promising results. However, there are no cross-disciplinary experimental studies combining the hygrothermal behavior and water quality performance of BioRoofs, generating large uncertainties on their overall performance. In this view, the current study combines the water quality assessment, hydrological behavior and thermal performance of BioRoofs. In particular, it compares the performance of a vegetated and a non-vegetated testbed irrigated with wastewater under a simulated Mediterrenean spring. A vegetated testbed, used as a control plot, was irrigated with tap water to compare and understand the influence of wastewater on the hydraulic properties of the BioRoof. The results revealed that the vegetation layer further increases the water retention capacity of the BioRoof due to the dry substrate that plant transpiration streams induce. Additionally, plants cut the temperature peaks by 20% and delay them by as much as 6 hours, providing extra heat insulation for buildings and improved urban microclimate if upscaled. Furthermore, the contribution of plants is singificant in the removal efficiency of reactive nitrogen, reducing by 61% the total inorganic nitrogen in wastewater. Overall plants are a sink for nutrients and induce strongly unsaturated conditions by reducing the water content in the BioRoof. The unsaturated conditions offer great potential for the removal of contaminants and further studies should exploit them in combination with the phytoremediation effect of plants.

Zusammenfassung

Bis 2050 werden 70% der Weltbevölkerung in Städten leben. Grüne Infrastruktur ist ein grundlegendes Instrument für eine nachhaltige Stadtentwicklung. Wenn man bedenkt, dass Dächer bis zu 50% der undurchlässigen Flächen in städtischen Gebieten ausmachen, bieten sie eine große Chance, natürliche Lösungen zu integrieren und vielfältige Ökosystemleistungen zu erbringen. BioDächer sind eine neuartige Technologie basierend auf der Kombination von Dachbegrünung und konstruierten Feuchtgebieten. Damit haben sie das Potenzial, nicht nur eine kostengünstige dezentrale Abwasserbehandlung zu bieten, sondern zugleich hygrothermischen Vorteile zu nutzen. Erste Studien deuten auf einen positiven Effekt der BioDächer auf die Wasserqualität von Abwässern hin. Jedoch fehlen interdisziplinäre experimentelle Studien, die das hygrothermische Verhalten und die Veränderung der Wasserqualität von BioDächern kombinieren, was zu großen Unsicherheiten in Bezug auf ihre Gesamtleistung führt. Daher kombiniert die aktuelle Studie die Bewertung der Wasserqualität, das hydrologische Verhalten und die thermische Leistung von BioDächern. Insbesondere vergleicht sie die Leistung eines bewachsenen und eines nicht bewachsenen, mit Abwasser bewässerten Testbeets unter simulierten mediterranen klimatischen Bedingungen. Um den Einfluss des Abwassers auf die hydraulischen Eigenschaften des Substrates des BioDachs zu analysieren und mögliche toxische Auswirkungen auf die Pflanzen zu beobachten, wurde gleichzeitig ein bewachsenes Testbeet als Kontrollfläche mit frischem Leitungswasser bewässert. Die Ergebnisse zeigen, dass die Transpiration der Pflanzen in der Vegetationsschicht die Wasserrückhaltekapazität des BioDachs stark erhöht. Darüber hinaus senken die Pflanzen die Temperaturspitzen um 20 % und verzögern sie um bis zu 6 Stunden, wodurch die Gebäude zusätzlich wärmeisoliert werden und BioDächer bei weitreichender Anwendung das Potenzial haben, das städtische Mikroklima zu verbessern. Darüber hinaus wurde durch die Pflanzen reaktiver Stickstoff effizient aus dem Abwasser entfernt, mit einer Reduzierung des gesamten anorganischen

Stickstoffs um 42 % für die bepflanzten Testbeete. Dementsprechend fungieren die Pflanzen des BioRoofs als Senke für Nährstoffe im Abwasser und können damit gegebenenfalls eine Wiederverwendung für den häuslichen Gebrauch als Betriebwasser ermöglichen.

Abbreviations

CR	Control (BioRoof plot)
CW	Constructed Wetland
ET	Evapotranspiration
GI	Green Infrastructure
GR	Green Roof
K	Kelvin
NVG	Non-Vegetated (BioRoof plot)
TP1	Temperature Point 1
TP2	Temperature Point 2
UHI	Urban heat island
VG	Vegetated (BioRoof plot)
WWTP	Wastewater Treatment Plant

Table of Contents

List of Figures

List of tables

1 INTRODUCTION

In a growing world population with increasing demand for food and water, current and future generations face multiple social, economic and environmental challenges. According to United Nations (2018) statistics, the world urban population is projected to increase by 2.5 billion between 2018 and 2050, consisting of approximately 70% of the total population. Historically, cities are known to be drivers of societal and economic growth, however unplanned urbanization can be detrimental for the three-dimensions of sustainable development: economic, social and environmental. The Food and Agriculture Organisationis estimates that 17 hectares of soil are lost every minute due to urban expansion (FAO, 2016). Sealing of urban soils with impervious materials is interlinked with climatic processes (Buyantuyev & Wu, 2010), water runoff (Mohammad & Adam, 2010) and biodiversity (Huang *et al.*, 2018). At the same time, the intensification and expansion of cities will demand a more sustainable and circular use of water. The generation of higher loads of municipal wastewater must be accommodated, while cities must deal with bigger demand for clean domestic water.

Soil sealing is the primary direct consequence of urban development. Impervious layers shift the natural water balance generating higher amounts and speed of water surface runoff, which increases the risk of floods. The increased frequency and intensity of surface runoff from urban areas combined with insufficient drainage systems, causes recurring severe flood events. Berndtsson *et al.* (2019) identified poor urban planning as the highest impact drivers for increased urban flood risks. The authors suggest that increased permeability and responsive engineering should be given high priority in urban planning. Furthermore, the decreased filtering capacity of the soil and the increase in the urban surface runoff, which is often discharged directly into waterbodies, causes deterioration of water quality.

The increasing density of urban conglomerations generates higher loads of municipal

wastewater, putting more pressure on the centralised wastewater treatment plants, which already face challenges due to unexpected extreme weather conditions and growing natural hazards (Jafarinejad, 2020). Holmes *et al.* (2019) concluded that in many wastewater treatment plants the reactive nitrogen from the wastewater is not removed prior to its disposal to the environment. The removal of reactive nitrogen in most treatment systems relies on complete nitrification-denitrification processes. Although such systems (e.g. activated sludge) can sometimes reach removal efficiencies up to 100%, the aeration to enhance biological oxidation of ammonia to nitrate (nitrification) requires large amounts of energy input (Holmes *et al.*, 2019), which does not make them economically or environmentally sustainable. In the USA, 35% of the municipal energy budget is used by water and wastewater utilities (U.S. Environmental Protection Agency, 2014). Other systems that do not require as much energy (e.g. partial nitrification-denitrification, simultaneous nitrification-denitrification) are only suitable for wastewater with specific characteristics (ammonia concentrations >500 mg L^{-1}, dissolved oxygen concentrations <0.5 mg L^{-1}) (Holmes *et al.*, 2019). The conventional treatment methods are either too energy intensive and expensive or inefficient to treat nitrogen from various types of domestic wastewaters, leading to pollution of rivers, coastal water and lakes. According to the European Environmental Agency (2018), 12% of all the European surface water bodies are subject to point source pollution from urban wastewater.

Excessive amounts of nitrogen in water have negative impacts on the environment and human health. For instance, high nutrient concentrations in water bodies combined with high energy input from solar radiation, trigger the algal growth. The algal bloom causes the reduction of sunlight availability and interferes with the productivity of aquatic plants and animals, water flow and temperature (Holmes *et al.*, 2019). On the other hand, the health risks associated with high nitrate concentrations in drinking water are well known. In particular, the most endangered group by water nitrate pollution is infants, which can develop infantine methemoglobinemia (aka blue-baby

syndrome) and the subsequent decrease of oxygen carrying capacity of the red blood cells (Hill, 2010; Holmes et al., 2019; WHO, 2011; Yamashita & Yamamoto-Ikemoto, 2014). Furthermore, the WHO (2011) has reported the potential carcinogenic character of high concentrations of nitrates in drinking water. It is therefore imperative to limit the nitrogen pollution of water bodies from domestic wastewater. Sustainable decentralised treatment systems in urban areas are necessary to enhance the reuse and recycling of wastewater for non-potable use (e.g. toilet flushing), in order to reduce the load on centralised wastewater treatment plants and minimize the domestic use of potable water.

Another major impact caused by urban sprawl is the urban heat island (UHI) effect, which was first described in the 1810s and has been since then directly linked with increased urbanisation and reduced green spaces (U.S. Environmental Protection Agency, 2018). It is described as the phenomenon in which the temperature of urban and suburban areas is elevated compared to the rural surroundings (U.S. Environmental Protection Agency, 2008). Urbanisation contributes to UHI mainly in two ways; by the active cooling from canopies and the heating due to the properties of urban materials. Trees and vegetation can yield a cooling effect by providing shade, which helps reduce the lower surface temperature, and through evapotranspiration (latent heat). In contrast, dry impervious materials used in cities reduce the shading and moisture that keep urban areas cool and increase surface temperature, warming the air which in turn circulates upwards via convection (sensible heat). Furthermore, urban materials have significantly different radiative properties (such as albedo and emissivity) than rural landscapes (U.S. Environmental Protection Agency, 2008). Urban areas typically have surfaces with lower albedo values resulting in more heat absorbance, which increases surface temperature and contributes to the UHI. Despite its early investigation by the meteorologist, Luke Howard, UHI is exacerbating and according to Levermore *et al.* (2017), from the late 1990s until 2016, the intensity of the UHI in the city of Manchester, UK, has increased. According to the authors' estimations, until the end of the century, an additional temperature

increase of 2.4 K (Kelvin) in Manchester will be accredited to this phenomenon. The U.S. Environmental Protection Agency (2008), estimates that the mean annual temperature of a city with one million inhabitants can increase by up to 12 K, compared to its surroundings. With higher urban temperatures and global climate change working synergistically, UHIs are expected to experience more frequent and severe heat waves in the future (Rizvi *et al.*, 2019), resulting in higher cooling energy demand and pollutants' emissions. Enhanced urban vegetation and green roof technologies are ways to mitigate the energy imbalance in urban areas and improve urban microclimate and air quality (Oke, 1982; U.S. Environmental Protection Agency, 2008; Imran *et al.*, 2018; Sanchez & Reames, 2019).

Hence, there is a need to invert the paradigm of urban planning and favor the transition towards an integrated and sustainable approach (i.e., mitigate-adapt-avoid-restore), which is typical of the Green Economy. Since 2013 the European Union has adopted a green infrastructure policy ('*Green Infrastructure – Enhancing Europe's Natural Capital'*) to demonstrate how EU-wide action can add value to the local initiatives towards sustainabe development; one of the main actors to provide environmental, economic and social benefits through Green Infrastructure (GI) is green roofs (European Commission, 2013). To the same view, the '*Green Infrastructure Guidance*' for UK's decision makers, planners and stakeholders considers green roofs a flagship of the development of GI (Natural England, 2009). Several cities have mandated the implementation of GI, while others offer financial incentives to promote them. For example, in London all new major development proposals must be designed to include green roofs and green walls, with the scope to increase the green roof coverage of the city (GLA, 2016). Similarly, all new buildings in Copenhagen with a slope less than 30^{o} must establish a green roof, as the Municipality of Copenhagen envisages to cover 200,000 m^2 of green roofs in the upcoming years. Lately, the leading role in the green roof strategy in Europe has been taken by Germany. Since 2015, the Hamburg Ministry of Urban Development and Environment allocated €3 million to encourage the construction of green roofs,

with the ambition to cover 70% of the city's suitable rooftops with vegetation (IFB Hamburg, 2020). Economic incentives are also given in Austria, where the Federal Ministry of Sustainability and Tourism grants up to 150€ m^{-2} for installation of green roofs on new and renovated commercial buildings. Similar measures have been adopted in other European countries as well as in North America (e.g. Canada, USA) and Asia (e.g. China, Japan). The lifecycle costs of green roofs can be retrieved in most of the markets around the world, and a widespread implementation would yield tremendous individual and social benefits and lower lifecycle costs (Feng & Hewage, 2018). There is an imperative need, strong political will and economic benefit to increase the resilience and adaptation of cities to urbanisation and climate change by implementing multi-purpose sustainable solutions, such as green roofs. Those solutions stem from the multiple benefits that the natural processes of green roofs offer to mitigate the environmental consequences of urban sprawling.

Green roofs (GRs) are able to retain and evapotranspirate stormwater, thus reducing the surface runoff and combined sewer overflows (Brunetti et al., 2016). Andrés-Doménech et al. (2018), demonstrated that over a 1-year period, an extensive GR was able to retain on average 65% of the rainfall volume, while a conventional roof only 13%. During the most intense rainfall event (125 mm), the runoff from the conventional roof was 119 mm (5% retention efficiency) and from the GR 55.8 mm - (55% retention efficiency). The literature on green roof hydrology reports stormwater retentions ranging from 36% to 94% (Hutchinson *et al.*, 2003; VanWoert *et al.*, 2003; Carpenter & Kaluvakolanu, 2011; Sims *et al.*, 2016). In a study conducted by Liu *et al.* (2019), an extensive vegetated GR with a similar substrate composition and depth to this study, reduced the surface runoff by 38%. Stormater peak flow attenuation is another hydrological benefit that green roofs provide. Sims *et al.* (2019) concluded that the average peak flow rate attenuation from rainfall events due to the installation of a green roof was 58%. Similarly, Brunetti *et al.* (2016) proved that an 8-cm extensive green roof was able to reduce the peak flow rate between 7% and 60%, depending on the initial water content of the substrate. Although these studies demonstrate the contribution of

green roofs in stormwater retention and attenuation of their peak flows, they were designed to emphasize their hydrological benefits and other environmental gains were not simultaneously investigated.

While the stormwater management is the bigger concern in wet climates, the multiple benefits of GRs provide moderation of high temperatures, especially in warm climates. Ávila-Hernández *et al.* (2020) investigated the energy performance of residential buildings with an extensive vegetated GR in eight cities in Mexico and demonstrated average indoor temperature attenuation up to 4.7 K with decreased energy consumption for cooling up to 46%. Similar findings were reported by Bevilacqua *et al.* (2020). In a study in Southern Italy, Gagliano *et al.* (2016) revealed that the vegetation layer reduced the peak outdoor surface temperature by 30 K and moderated the daily temperature fluctuations by a factor of 6, compared to a conventional roof. Other research on the thermal behaviour of GRs in buildings has proven that the addition of vegetation exhibits significant heat-stress reduction during summer months (Ziogou *et al.*, 2017; Cascone *et al.*, 2018; Castiglia & Wilkinson, 2019). Nevetheless, the thermal benefits of green roofs are not limited to the building-scale. In an exhaustive review, Susca (2019) reported that vegetated green roofs, irrespective of their configuration, are beneficial in mitigating UHI in the roof level of all the investigated climates. The review also concludes that in order to mitigate UHI in pedestrian level, the deployment of green roofs in urban-wide scale is essential. A study of the New York City's heat effect found that increasing green roofs reduces the surface temperature of the city by 0.4 K on average and by 0.7 K at 3pm when the temperature tends to be highest (Rosenzweig *et al.*, 2009). In another urban-scale study, Dong *et al.* (2020) empirically quantified the cooling effect of green roofs in southern China using remote sensing and concluded that implementing 500,000 m^2 of green roofs within 2 years, decreased the average land surface temperature by 0.91 K. Consolidating the findings on the themal and hydrological performance of several configurations of extensive green roofs, it can be pressume that they have a positive effect in the livelihoods of urban communities. However, the

conclusions are incomprehensive as the studies have focused on the performace of green roofs on one of the aspects (hydrological or themal) using different substrates, plants and environmental conditions. The green roofs can simultaneously provide multiple ecosystem services and research must be inclusive to assess their full potential.

Considering that rooftops represent up to 50% of the total impervious surfaces in urban areas, GRs provide a great opportunity to integrate the natural processes in treatment systems, such as that of Constructed Wetlands (CWs) (Zapater-Pereyra *et al.*, 2016) in order to reduce the load on centralised wastewater treatment plants and allow the reuse of water for non-potable purposes. CWs are an alternative treatment system with comperable nitrogen removal efficiencies to the conventional systems (e.g. activated sludge) (Vymazal, 2018). Due to their reliance on the natural processes that occur in wetlands they require negligible energy input, relatively simple configurations and low operation/maintenance costs. Masi *et al.* (2017) demonstrated how the implementation of a decentralized CW system for combined sewer overflow treatment was able to significantly reduce pollutant loadings on water bodies, thus drawing the attention on the need to develop similar systems for the optimization of the urban drainage systems. According to Song *et al.* (2013), if water depths are designed within the weight-bearing capacity of rooftops (under 30 cm), CWs can be incorporated into urban planning. In a comprehensive review of the role of constructed wetlands in the recycling and reuse of greywater, Arden & Ma (2018), concluded that green roofs have the potential to be a cost effective, low-energy method to produce non-potable water. The study reported that GRs achieved a reduction of 71% to 84% of Total Suspended Solids (TSS), Biological Oxygen Demand (BOD) and Turbidity. A system that combines green roofs and constructed wetlands, which in this study is referred to as BioRoof, is able to 1) retain, delay and evapotranspirate stormwater, 2) reduce the energy consumption of the building by maximizing the evaporative cooling effect induced by the continuous feeding of the BioRoof, 3) diffusively treat wastewater through a combination of microbial processes and plant's detoxification. Zapater-

Pereyra *et al.* (2016) demonstrated that a horizontal flow BioRoof in the Netherlands was able to retain 62% of the total inflow volume, while significantly improving the water quality in the effluent (87% reduction of total nitrogen). However, the BioRoof's substrate was covered with a turf mat that was previously grown in a highly fertilised soil, which would increase the costs for a widespread implementation of BioRoofs. Additionally, due to the specific weather requirements of turf mats, they are not commonly used in BioRoofs located in climates with longer warm and dry periods. Most studies on the treatment efficiencies of BioRoofs have used macrophytes and other plant species suitable for tropical and wet climates (Van *et al.*, 2015; Vo *et al.*, 2017, 2018). Research on treatment efficiencies of plants that are suitable for BioRoofs in regions with warm and dry seasons is scarce. Therefore, there is a lack of understanding of the opportunity that BioRoofs offer to reduce heat waves and water surface runoff, while harnessing the great redox potential to treat domestic wastewater in warm and dry climates, such as the Mediterrenean.

To this view, the current study provides a cross-disciplinary plot-scale investigation of the environmental benefits of BioRoofs under Mediterrenean climatic conditions. In detail, the role of typical green roof plants on the hydrological behavior, the heat transport within the BioRoof and the inorganic nitrogen concentration in the effluent are evaluated by comparing a non-vegetated and a vegetated BioRoof irrigated with wastewater. Additionally, the short-term effects of the wastewater on the hydraulic properties (i.e. bioclogging) of the BioRoof and other possible inteferences caused by the organic load, such as stimulation of plant growth or any toxic effects are assessed. For this purpose, a third testbed that consis conditions. The results expand the current knowledge on the benefits of BioRoofs with similar setups and climatic conditions, while providing guidance for future research on their optimization as emerging sustainable solutions in cities.

2 MATERIALS AND METHODS

2.1 *Experimental setup*

The experimental setup was designed to meet the specifications of extensive green roofs, which are typically light weight, with little to no maintenance and their substrate depth does not exceed 20 cm (Oberndorfer *et al.*, 2007; FLL, 2008).

2.1.1 Green Roof plots

Three experimental plots were used in the current study, with the same material, substrate composition and sensors. Each plot consisted of a plastic box with length width height dimensions: 36 cm x 57 cm x 15 cm. A 12-cm layer of artificial soil (ROOF SOIL 2, DAKU ITALIA srl.) was placed on top, to allow the infiltration of water and provide a growing medium for the plants and the bacteria, as well as a surface for the adsorption of nutrients. The artificial soil, which consisted of a mixture of volcanic minerals (lapillus lava and pumice stone) for good aeration and drainage and a peaty composted soil improver (KOMPOST, DAKU ITALIA srl.), had a measured porosity and bulk density of 0.66 and 0.89 g cm^{-3} respectively. The mixture of peat soil and volcanic minerals has been identified as the most effective in stormwater retention, without compromising the thermal benefits of the BioRoof (Sandoval *et al.*, 2015; Liu *et al.*, 2019). Additionaly, the substrate is typically used for BioRoofs and due to the relatively coarse texture and high hydraulic conductivity, it should remain highly unsaturated providing oxic conditions for the growth of nitrifying bacteria. Below the substrate, a 3-cm drainage layer consisting of coarse gravel provided additional water retention and ensured good drainage and aeration of the BioRoof's substrate. A highly permeable non-woven blanket, commonly known as geotextile, was used as the filter layer which prevented the small particles from being washed out from the substrate into the drainage layer or out of the

system. The substrate was carefully compacted during the assembly to simulate real BioRoof conditions, and minimize soil heterogeneities. The BioRoofs were placed on top of a wooden frame with a small inclination (≈1%) to assist the drainage with gravitetional potential. A schematic representation of the BioRoof boxes is illustrated in Figure 1.

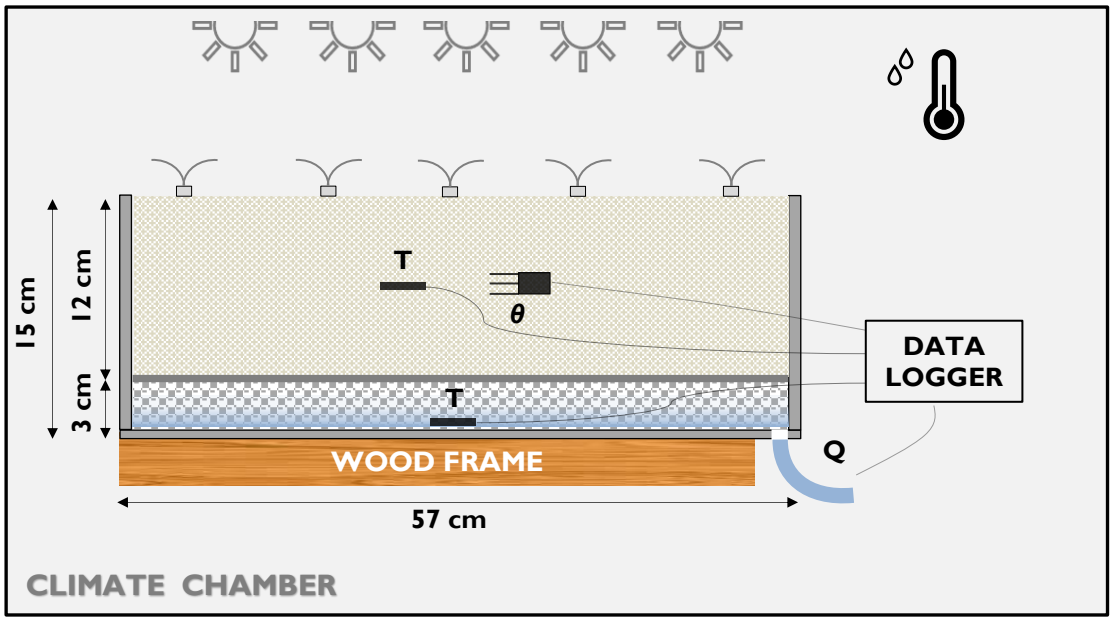

Figure 1. Schematic representation of the configuration of sensors in the three testbeds. Grey lines on the BioRoof substrate indicate irrigation by capillary pipes (θ: Stevens HydroProbe sensor, T: Thermocouples, Q: Outflow)

The experiment consisted of three testbeds; two were irrigated with a 1:1 diluted wastewater (VG and NVG in Figure 2) and the third testbed, which served as the control plot, was irrigated with tap water (CR in Figure 2). The difference in the two testbeds treated with wastewater was the soil coverage; VG (as well as CR) had a layer of vegetation cover while the substrate of the NVG was directly exposed without the addition of plants. Observed differences between the vegetated and non-vegetated BioRoofs will highlight the role of the plants in the hygrothermal behavior of the BioRoof and the removal efficiency of inorganic nitrogen. Significant differences in the vegetated and control testbeds might reveal changes in the the hydrological behavior of the BioRoof due to the rapid growth of the microbial community on the surface of the sustrate (e.g. bioclogging) and other effects (e.g. plant growth or toxicity) induced by the injection of wastewater. A schematic

representation of the elements of the testbeds can be found in Figure 2. The black lines on top of the BioRoof's substrate indicate wastewater irrigation (VG and NVG), while the blue lines in the CR indicate injection of tap water.

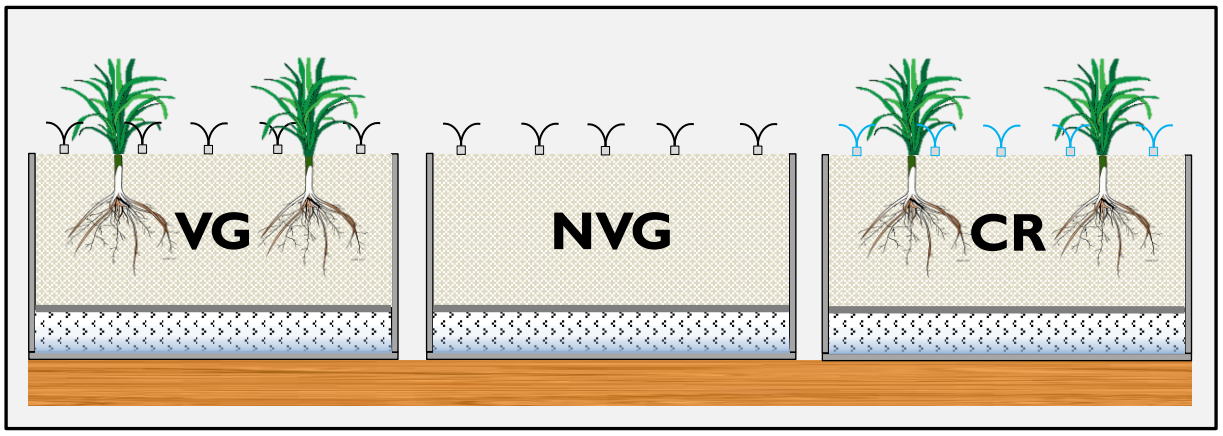

Figure 2. Schematic of the experimental setup (VG: Vegetated, NVG: Non-Vegetated, CR: Control). Black lines: wastewater irrigation, blue lines: tap water irrigation

2.1.2 Irrigation system

Figure 3. Multi-drip outlet irrigation system of two experimental plots connected with T-splitter (left: vegetated, right: non-vegetated).

The artificial irrigation system delivered a 1:1 diluted wastewater (≈75 mgCOD L^{-1}) and tap water to the surface of the substrate, using multiple drip-outlets. The irrigation in the two experimental plots treated with wastewater was realized with the use of an electric submersible pump, which was connected to a network of tubes that diverged using a T-splitter and finally

delivered the dilutant with drip outlets (Figure 3). Due to the nature of the pump, elevation head had to be manually adjusted in order to ensure constistent hydraulic head and flow rate in the plots. The artificial irrigation system in the control plot was set up differently than the other two experimental plots. A peristaltic (or centrifugal) pump with 16 channels delivered consistent flow rates regardless of the hydraulic pressure. The capillary tubes from the channels were connected in pairs in 2 levels; the final connection resulted in 4 tubes delivering the tap water via multiple drip outlets to the surface of the soil substrate (Figure 4).

The irrigation schedule was designed to: 1) simulate the real operating conditions of BioRoofs, 2) induce an alternation of wet and dry soil conditions, and 3) minimize the plant water stress. In particular, each box was irrigated four subsequent days per week for one hour, during which 3 L of tap water (CR in Figure 2) or diluted wastewater (VG and NVG in Figure 2) were distributed on the soil surface. As shown in Brunetti *et al.* (2018), such irrigation pattern can significantly enhance the evaporative cooling efficiency of green roofs. In the following 3 days of the week the testbeds remained dry. During weeks 1 and 6, tracer experiments were conducted and the amount of water/wastewater injected was doubled (6L) to speed up the recovery of the tracer without idling the monitoring campaign.

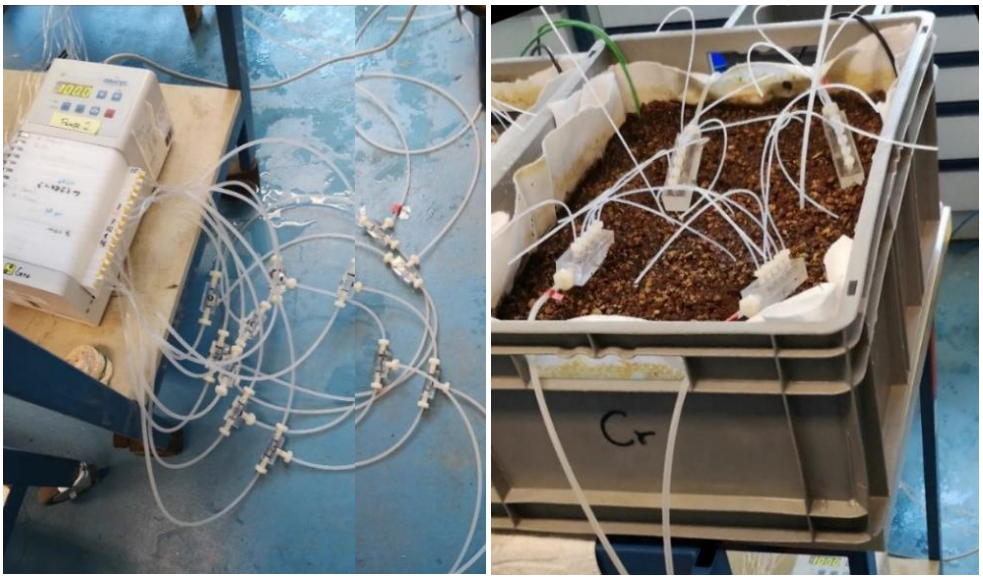

Figure 4. Irrigation system in the control plot (Left: Two-level parallel connection of capilarry pipes from the peristaltic pump, Right: Multi-drip outlets delivering the water near surface)

2.1.3 Plants

In the two testbeds with plants (VG, CR) it was important to select species that are typically used in extensive green roofs and urban green spaces which are native or compatible to the Mediterrenean climate but also require minimum maintenance. A mix of Alyssum (*Lobularia Maritima* or *Alyssum maritimum*) and Cheddar Pink (*Dianthus Gratianopolitanus*) were selected due to their resistance in wide range of soil moisture conditions, adaption to high air temperatures and low maintenance. The alyssum and dianthus thrive in soils with good aeration and drainage, making them a good match for the experiment.

Lobularia Maritima are flowering subshrubs that belong to the genus of *Alyssum* in the family *Brassicaceae*, with richest species diversity in the Mediterrenean. They are common in sandy beaches and dunes, but also grow on cultivated fields as a groundcover and on walls and are native to south-eastern France and southern Spain[1]. They grow up to 30 cm in height and width with evergreen foliage and can be planted in loamy, chalky or sandy soils as long as they are well-drained and are tolerant to soil pH, heat and drought[2]. *Dianthus gratianopolitanus* is a herbaceous everegreen perennial in the family *Caryophyllaceae*, native to southern Europe and Asia[3]. It grows up to 20 cm and thrives in sandy and loamy well-drained soils with slightly alkaline to neutral pH and sunny to partial shady conditions[4]. Both species are tolerant of urban pollution and thrive in city environments. Two plants of each species were planted in a diamond-shaped formation in the testbeds.

2.1.4 Climatic conditions

The BioRoofs were subjected to fully controlled climatic conditions during the experimental campaign. The climatic chamber Vötsch BioLine VB 1514 (Vötsch Industrietechnik GmbH,

[1] https://en.wikipedia.org/wiki/Lobularia_maritima. Accessed: 05.07.2020
[2] https://www.rhs.org.uk/Plants/137391/i-Lobularia-maritima-i-Snowdrift/Details. Accessed: 05.07.2020
[3] https://en.wikipedia.org/wiki/Dianthus_gratianopolitanus. Acccessed: 05.07.2020
[4] https://www.rhs.org.uk/Plants/5722/i-Dianthus-gratianopolitanus-i/Details. Accessed: 05.07.2020

Germany) was used to simulate typical Mediterrenean spring conditions (Figure 7). In particular, the air temperature, relative humidity, and the day/night alternation were set to replicate measured data from a weather station in southern Italy (39.33° N, 16.18° E). Unfortunately, the radiation intensity was not simulated or measured in the climate chamber.

Table 1. Controlled conditions in the climate chamber

Condition	Minimum	Mean	Maximum
Day (h)	12.5	13.6	15
Night (h)	11.5	10.4	9
Air Temperature (°C)	9	21	36
Relative humidity	24%	58%	94%

The prevailing climatic conditions during the monitoring campaign were: 12.5/11.5 h to 15/9 h (light/dark) photoperiod, at 9 °C to 36 °C and 24% to 94% relative humidity. Table 1 gives more information on the range of the climatic conditions, while temporal variations of the simulated environmental conditions (illumination, inflow rate, relative humidity, ambient temperature) are illustrated in Figure 5.

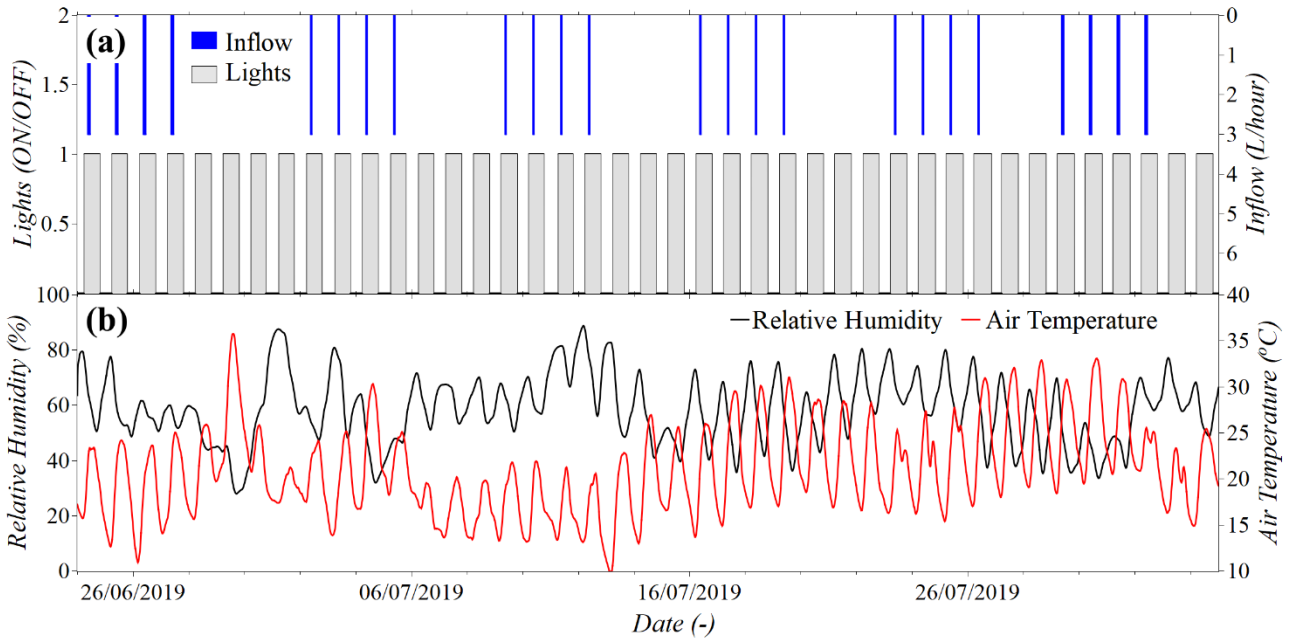

Figure 5. (a) Inflow rate (blue) and illumination pattern (grey); (b) Measured relative humidity (black line) and air temperature (red line)

2.1.5 Timeline

The experimental campaign consisted of several phases, which can be divided in two periods: the pre-monitoring, where all the necessary actions to initiate the data acquition were undertaken and the monitoring period when data was registered and used for analysis and interpretation (Figure 6). During the equilibration phase (Figure 6), the testbeds were subjected to the same environmental conditions and irrigated with tap water simultaneously in order to achieve homogeneous initial conditions. With the beggining of the first tracer test, the monitoring campaign was initiated, and it concluded at the end of the second tracer test (Figure 6). During the monitoring campaign, outflow samples were collected twice or three times per week and the inorganic nitrogen species were analyzed in the laboratory. While the tracer experiments were conducted, outflow samples were collected in small intervals and salt measurements were taken with an EC probe, while Deuterium in permill was measured with laboratory equipment and was later converted into concentrations (see 2.5.1 Isotope analysis). A full schematic of the timeline can be seen in Figure 6.

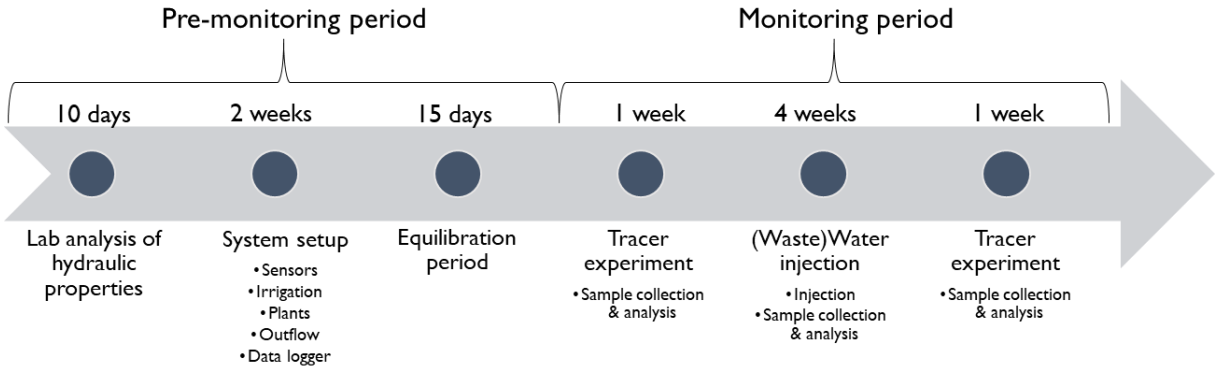

Figure 6. Schematic of the study's timeline

2.2 *Characterization of the Hydraulic Behaviour*

2.2.1 Transient Water flow

The collection of data during the monitoring campaign was achieved with an assembly of sensors that were connected with the data logger at the monitoring station (Figure 8). The monitoring setup

allowed the collection of information related to the climatic conditions and the transient water flow. Coaxial impedance dielectric reflectometers (Stevens HydraProbe) were placed in middle (*z*= -6 cm) of the substrate layer (Figure 1). An equidistant position from the upper and lower substrate boundary as well as the walls of the plot is the most representative to characterize the hydraulic behavior of the substrate. The HydraProbes are capable of measuring the real dielectric permittivity, the volumetric water content, the bulk electrical conductivity, and the temperature. A substrate-specific calibration curve was developed in the laboratory to link the measured soil permittivity to the actual volumetric water content (Seyfried *et al.*, 2005; Kargas *et al.*, 2013).

Figure 7. Vötsch BioLine VB 1514 climatic chamber

Figure 8. Data logging station

A small outlet at the end of each plot was connected to a tipping bucket through a tube (Figure 9). The tipping bucket is a typical rain gauge consisting of a funnel that directs the flowing water into a small seesaw container. After a known amount of water (5 mm) is collected in the seesaw container, the lever tips sending an electrical signal to the data logger station (Figure 8). Every minute, the data logger registers the number of tips that were sent as electric signals and thereby the outflow volume and rate can be determined. From the tipping bucket, the outflow was diverted outside the climatic chamber in seperate collection tanks, where the sampling was done (Figure 10).

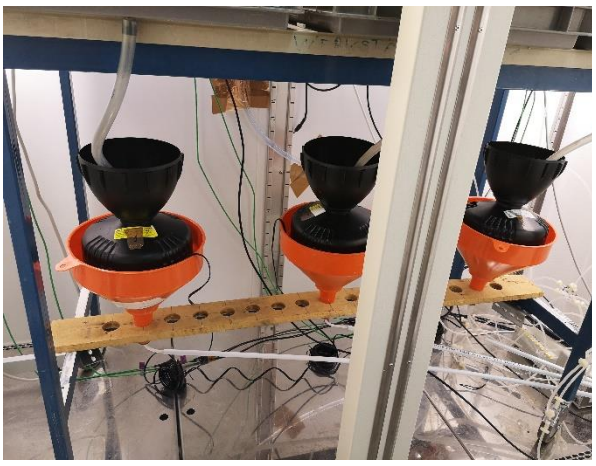

Figure 9. Tipping buckets - outflow measurement station

Figure 10. Final outflow collection and sampling station

2.2.2 Tracer Experiment

Tracer experiments were conducted twice to characterize the water and solute transport in the BioRoofs; once at the beginning and once at the end of the experimental campaign. From the analysis of the tracer samples we reconstructed breakthrough curves, which describe the concentration of the solute tracer in the outflow over time. Differences between the tracer curves of the two experiments could indicate alteration of the effective porosity of the susbtrate due to accumulation of biofilm from wastewater or preferential flowpathes along the living plant roots. The first tracer experiment was initiated in all three plots on June 24th, 2019 at 09:00. A known amount of deuterated water (1 mL, 90atom% deuterated water) and salt (30 g NaCl) was injected in all testbeds together with tap water (6 L) in the control plot, while a mix of wastewater and tap water in a 1:1 proportion (6 L) was used for the two test boxes. The same irrigation pattern (6 L day^{-1}) was applied for the following days, until the concentration of the salt in the outflow almost reached the background concentration. As mentioned previously, the amount of irrigation was doubled during the tracer tests to speed up the recovery of the tracers. The first test lasted 4 irrigation cycles (4 days and 24 L in each testbed). With the same procedure the second tracer experiment was conducted 5 weeks later (July 29th, 2019), which also lasted 4 irrigation cycle (days).

The collection of the outflow in both experiments was done in 50 mL plastic vials, with equal intervals (15 minutes), until the outflow was negligible (less than 5mm h^{-1}). The concentration of salt was measured using an electrical conductivity (EC) probe. Afterwards, an initial salt concentration curve was constructed for each box. Fifty subsamples for each box were taken for the isotopic analysis of the deuterated water.

2.3 *Characterisation of the heat transport*

In order to estimate the heat gradient of the testbeds, the experiment comprised of two temperature measurement points. A set of thermocouples was placed in Temperature Point 1 (TP1), the middle of the growing medium (z= -6 cm). An equidistant position to the upper and lower boundaries of the substrate, as well as the sidewalls of the plot is the most representative location for the characterization of the heat tranfer in the top layer. The second set of thermocouples was layed in Temperature Point 2 (TP2), on the bottom of the drainage layer (z= -15 cm). This will allow the comparison between the thermal conductivities and storage of the different layers. A high-precision thermometer was used to calibrate thermocouples, which were connected to the data logger with an acquisition frequency of 1 minute. A thermometer and humidity sensor of the climatic chamber were measuring the climatic conditions (ambient temperature and relative humidity) with a 1 minute resolution.

The characterization of the heat transport in the BioRoof is of crucial importance to assess its potential effects on the energy balance of the building and on the chemical and biological reactions in the growing medium (e.g. nitrification). The simulation of Mediterranean conditions in the climate chamber with significant temperature fluctuations was expected to emphasize the benefits and the limitations of BioRoofs on the energy balance. Furthermore, significant temperature differences were expected between the vegetated and the non-vegetated boxes due to the shadowing effect of the plants on the soil surface.

2.4 *Characterisation of the Reactive Nitrogen Transport*

Inorganic nitrogen compounds (ammonium, nitrite, nitrate) were monitored weekly in the outflow of all treatment boxes. To ensure reliability of the data, sampling was done two days per week with 2 to 3 samples daily in random timing relative to the irrigation cycles. The sampling, as well as the laboratory analysis, were done in replicates to minimize errors and avoid outliers. Plastic 50 mL vials were used for sampling and samples were stored in the fridge for a maximum of 3 days, due to the unstable nature of the inorganic nitrogen species. Variations in the concentration of reactive nitrogen between the control plot and the other plots would be mainly attributed to the high input of nitrogen from the wastewater. Deviations within the test plots would demonstrate the impact of the vegetation on the nitrogen balance. Total Inorganic Nitrogen (ammonium, nitrite and nitrate) concentrations in the injected wastewater and tap water were measured once in the middle of the experimental campaign.

2.5 *Analytical Methods*

2.5.1 Isotope analysis

For deuterium analysis, samples were analyzed with laser spectrometry (L 2140-i, Picarro Inc., Santa Clara, CA, USA). This method (Cavity Ring-Down Spectroscopy) provides very high-precision measurements of isotopic values, with a guaranteed 0.1 permil precision (1σ) and a 24-hour drift of 0.8 permil for δD (Picarro, 2014). According to the specifications of the instrument, the memory error is guaranteed to be less than 2% of δD after the 4^{th} injection.

In order to diminish the memory effect and attain more precise measurements, the Picarro L2140-*i* was set to 11 subsequent injections and the last 3 were averaged as the mean concentration of the sample, during post-processing analysis. For calibration, 3 samples with known isotopic concentrations (standards) were measured before a batch of 10 samples. From Picarro's user interface, datasheets with all measurements were exported and converted to mg L^{-1}. The last 3

sample replicates were averaged and the ratio of deuterium (δ^2H in ‰) relative to the Vienna Standard Mean Ocean Water was calculated from the local calibration curve (regression line). One reference sample (USGS50) and two standards with a known stable hydrogen isotopic composition of -47.9 ‰ and -77.2‰ were used for the configuration of the regression line. The concentrations (C) are finally expressed in mg L^{-1} using the following equation (Becker & Coplen, 2001):

$$C\ [mg\ L^{-1}] = 34.82\ [mg\ L^{-1}] \quad \times \quad \frac{1000 + \delta^2 H\ [‰]}{1000}$$

2.5.2 Measurement of Nitrogen Species

The measurement of the inorganic species of nitrogen was done in a UV-VIS spectrophotometer. In order to reduce the possible interference of the dissolved organic matter, all the samples were filtered through 0.1 µm Savana® Lab Disc membrane filters and stored for up to 3 days at 4 °C, without acid preservation. The ammonium and nitrite were measured colorimetrically. The determination of ammonium is based on the reaction with phenol and hypochlorite, to give an indophenol blue in an alkaline medium (Berthelot reaction). After the sample preparation, a 30 min reaction time is necessary before measuring the absorbance at 676 nm. The nitrite determination is based on the reaction of nitrite in acid solution of a primary amine (Sulphanilamide), to form diazonium salt which is coupled to an aromatic amine to produce the red azo dye, whose absorbance can be measured at 540 nm.

Generally, the determination of nitrate is difficult because of the high probability that constituents will be present, interfering with the absorbance of nitrate at certain wavelengths. The conventional methods that are most commonly used for uncontaminated waters measure the absorbance of nitrate between 220 and 275 nm. Due to the nature of the samples, the absorbance of UV by the organic matter interfered with the nitrate, hence another method had to be employed for its measurement. The second-derivative ultraviolet spectrophotometric method (SDUV) is

proposed by the Committee of Standards Methods for the Examination of Water and Wastewater, members of the American Public Health Association, (APHA), American Water Works Association (AWWA) and Water Environment Federation (WEF). Quality checks indicate that the SDUV method is the most accurate for the measurement of nitrate in wastewater samples (Ferree & Shannon, 2001). All samples and standards were treated in the same way; 5 mL of sample (or standard) was transferred into it a glass vial and mixed thoroughly with 1 mL of sulfuric acid (H_2SO_4), to reduce the pH. Subsequently, the absorbance of each sample (or standard) was measured in the range of 220 and 230 nm in the spectrophotometer and the maximum second derivative was calculated in a computer interface. By calculating the maximum second derivative of the standard samples in the wavelength of 220 and 230 nm, we drew a calibration curve (R^2>0.99). From the measured standards, a regression line was induce; from which maximum second derivative of all the samples can be translated into concentrations. The accuracy of this method is higher than 0.5 mgN-NO_3^-/L and the standards used were 0.5, 1, 1.5, 2.5, 4 and 6 mg L^{-1} N-NO_3^-.

3 RESULTS AND DISCUSSION

3.1 *Characterisation of the hydraulic behaviour*

3.1.1 Transient Water Flow

Figure 11 shows the measured volumetric water content (θ) in the substrate of the three testbeds during the experimental campaign (a) and draws an example of the differences observed in θ and the subsuface flow between the vegetated and non-vegetated plots (b and c). In particular, the non-vegetated BioRoof exhibits a higher average soil moisture ($\overline{\theta}$ = 0.29), while the vegetated ($\overline{\theta}$ = 0.25) and control ($\overline{\theta}$ = 0.26) remain slightly more wet (Table 2). This tends to narrow and amplify during wet and dry periods respectively, as is clearly shown in Figure 11b which reports the comparison between the volumetric water contents during July 16th after four days without wastewater injection. The soil moisture difference at the beginning of the irrigation is almost 0.06, which leads to an anticipated and higher outflow (Figure 11c) in the non-vegetated BioRoof. In particular, the outflow in the vegetated testbed starts approximately 25 minutes later and its peak is 25% lower. On the other hand, the moisture difference reduces to 0.03 during the injection and the hydrographs tailings are almost overlapping.

Table 2. Mean, maximum and minimum values of the measured volumetric water content in the three testbeds

θ ($cm^3\ cm^{-3}$)	Vegetated	Non-Vegetated	Control
Mean	0.25	0.29	0.26
Maximum	0.34	0.38	0.4
Minimum	0.16	0.24	0.2

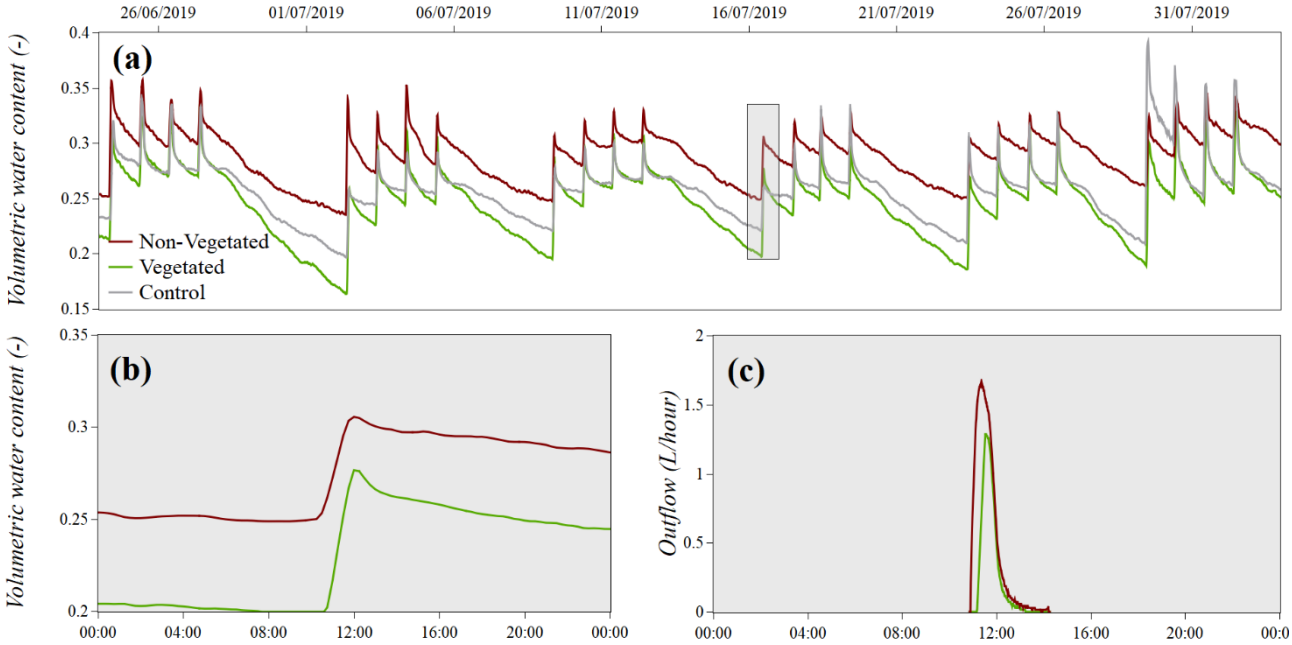

Figure 11. Hydrological behavior of the vegetated (green lines) and non-vegetated (brown lines) BioRoofs: (a) Measured volumetric water content in the substrate during the whole experiment, (b) Measured volumetric water content in the substrate during July 16th, (c) Measured outflow during June 16th

During dry periods, the average reduction of the volumetric water content in the vegetated was 14% and in the non-vegetated 10%, highlighting the contribution of plant transpiration in the water balance. In the non-vegetated BioRoof, the atmospheric conditions control the evaporation rate as long as the moisture content near the soil surface is sufficiently close to saturation. However, when the surface dries the atmospheric effect decreases drastically and evaporation is then controlled mostly by the rate at which water is able to move to the surface through the soil profile. This is also referred to as the falling rate stage (Brutsaert, 2014). During this stage, the capillary rise effect, which depends on the hydraulic characteristics of the porous medium, controls the bare soil evaporation. However, BioRoofs substrates are characterized by coarse textured soils, which limits the evaporation fluxes. Such behavior is less evident in the vegetated BioRoof due to multiple effects of the vegetation: 1) Plants induce the root water uptake in the substrate, thus reducing the soil moisture, 2) the vegetation cover mitigates the formation of the dry soil layer near the surface, which may disconnect the liquid continuity through the soil profile (Balugani *et al.*, 2018). Although the different hydrological behavior of the BioRoofs can be explained by the effects of the

vegetation, the positioning (i.e. depth) of a single moisture sensor in each of the three testbeds cannot eliminate a possible experimental uncertainty. Further experiments should incorporate more sensors in different depths to validate those findings.

Cumulative influx and bottom outflux are illustrated in Figure 12. The step-like gradient in the cumulative outflow indicates that the green roofs have an immediate response to the irrigation with a negligible delay in the hydrograph. Total injection volume is 96 L in the control testbed and 192 L in the vegetated and non-vegetated combined. For practicalities we assume that the 192 L in the combined wastewater tank were distributed equally in VG and NVG. Interestingly, the total outflow volume is highest in the driest testbeds – vegetated (70 L) and control (62 L) – while the more moist non-vegetated (60 L) exhibited the lowest outflow. Those differences might have been induced due to the sensitivity of the wastewater injection system to hydraulic loses, potentially leading to unequal distribution of the influent. Despite that, all three BioRoofs exhibited high evaporation (and transpiration) rates; loses to vapor accounted for 27-37% of the total volume of injection. Due to the possible bias introduced in the cumulative hydrographs of the vegetated and non-vegetated BioRoofs, a more thorough analysis of influxes, outfluxes and water retention will be presented solely for the control plot.

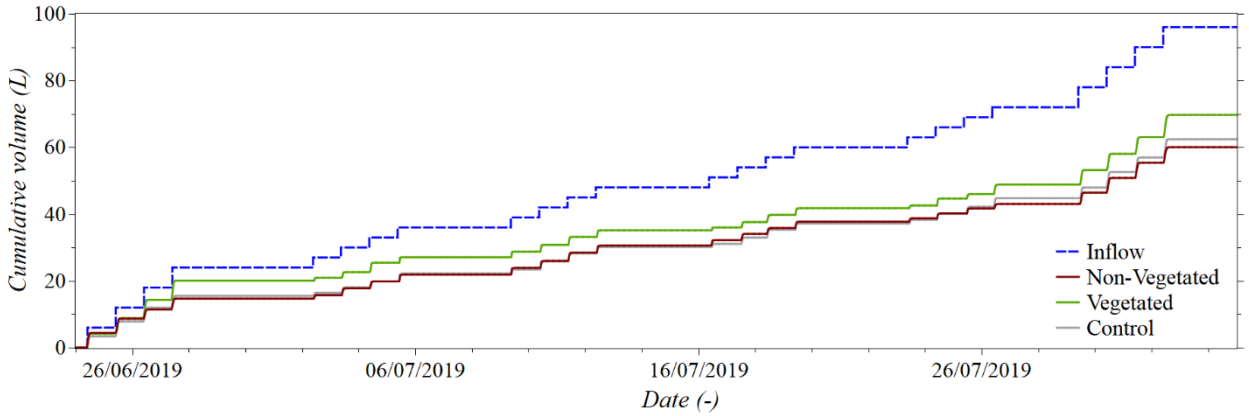

Figure 12. Cumulative hydrographs of influx (blue dashed line) and outflow from the three BioRoofs (red, green and grey lines) during the monitoring campaign.

Figure 13 presents the daily inflow and outflow rates from the control plot during the first

(top row) and last (bottom row) irrigation cycle for 4 out of the 6 weeks. A delay of the outflow is observed, ranging from 15 minutes to just above 2 hours (July-29), depending of the initial substrate moisture. The difference between the areas of the inflow and outflow curves in Figure 13 represent the water that was retained by the BioRoof and was lost to evapotranspiration. The daily water retention ranges from just over 9% (Aug-01) to approximately 70% (July-02). It is evident that the outflow during the first irrigation cycles (top row) is lower compared to the last day (bottom row). This trend is aparent during the whole monitoring campaign in all testbeds. The average outflow rate from the CR was 1.3 L h^{-1} with a maximum of 2.7 L h^{-1}, which was recorded twice during the last week (tracer experiment) when highest soil moistures were recorded. The environmental conditions and the average hydrological response of the BioRoof related to the the irrigation cycles (days) are reported in Table 3.

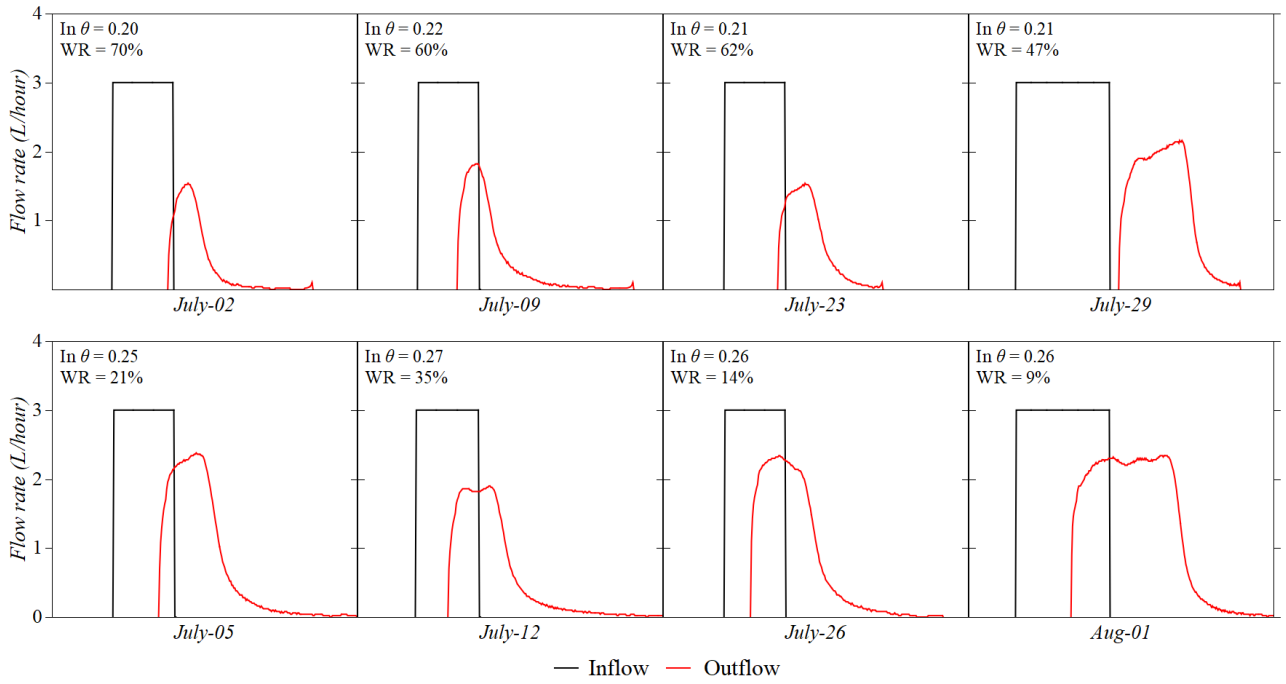

Figure 13. Hydrograph of daily inflow (black line) and subsurface flow (red line) of the control plot. Top-row: the first irrigation cycle (day) of weeks 2, 3, 5 & 6; Bottom-row: the last irrigation cycle of weeks 2, 3, 5 & 6. Inset: Initial volumetric water content prior to the beginning of the irrigation cycle (In θ) and daily water retention (WR).

On a 6-week average, the 1st cycle (day) of the week retained 59% of the injected volume, followed by 31%, 30% and 28% on cycles 2, 3 and 4 respectively. During the first day of the 6-

week average, the volumetric water content prior to the beginning of the irrigation cycle and the air temperature were at their lowest. Despite the low temperatures, the initial moisture conditions are the determining factor that increase water retention capacity. A Pearson Correlation Coefficient (PCC) test on the daily data revealed that among all factors only the initial θ was strongly correlated to the water retention (ρ= -0.73). Similar findings have been reported by other studies on the hydrological performance of green roofs (Sandoval *et al.*, 2015; Brunetti *et al.*, 2016; Andrés-Doménech *et al.*, 2018; Sims *et al.*, 2019).

Table 3. Prevailing atmoshepric conditions and hydrological response of BioRoofs averaged by irrigation cycle (day) of each week. (WR: water retention, Initial θ: volumetric water content prior to the beginnig of the irrigation cycle, T: temperature)

Irrigation cycle	WR	Initial θ ($cm^3\ cm^{-3}$)	T (°C)
1	59%	0.22	24
2	31%	0.27	25
3	30%	0.26	26
4	28%	0.26	25

When the hydrological data are grouped by the amount of irrigation applied (6 L day^{-1} during weeks 1 & 6 and 3 L day^{-1} during weeks 2, 3 & 4), the correlation of water retention to the initial θ is stronger when less water is applied (ρ= -0.83) and weaker when the amount of water was doubled (ρ= -0.57). This can be explained by the high permeability of the BioRoof substrate near its field capacity; a point that significantly decreases the water retention (Sims *et al.*, 2019). Table 4 shows the atmospheric conditions and the hydrological response of the BioRoofs averaged per week. The highest weekly average water retention occured during the 2nd week of irrigation (July-02 to July-05), when the initial soil moisture was the lowest (θ= 0.24). Despite the high temperature during week 6, the water retention was the lowest throughout the monitoring campaign, mainly due to the higher hydraulic load (6 L day^{-1}). Nevertheless, more than a quarter of the irrgation applied exited the system as water vapor. Although the initial water content during week 3 (θ= 0.25) was the same as weeks 4 and 5, the water retention was lowest. This is attributed to the higher average temperature

(6-7 K), generating available water storage in the BioRoof (Sims *et al.*, 2016).

Table 4. Prevailing atmoshepric conditions and hydrological response of BioRoofs averaged by week (WR: water retention, Initial θ: volumetric water content prior to the beginnig of the irrigation cycles, T: temperature)

Week	WR	Initial θ ($cm^3\ cm^{-3}$)	T (^oC)
1	35%	0.27	23
2	44%	0.24	24.2
3	34%	0.25	20.3
4	43%	0.25	27.4
5	37%	0.25	26.2
6	27%	0.26	28.8

3.1.2 Tracer experiment

Figure 14 reports the normalized salt and deuterated water concentration in the outflow measured at the beginning (top) and the end (bottom) of the experimental campaign. The x-axis is normalized by dividing the cumulative outflow with the mean outflow rate. The tracer concentration curves for salt and deuterated water are similar, as expected for coarse, unsaturated substrate indicating advection and dispersion are the dominating transport processes.

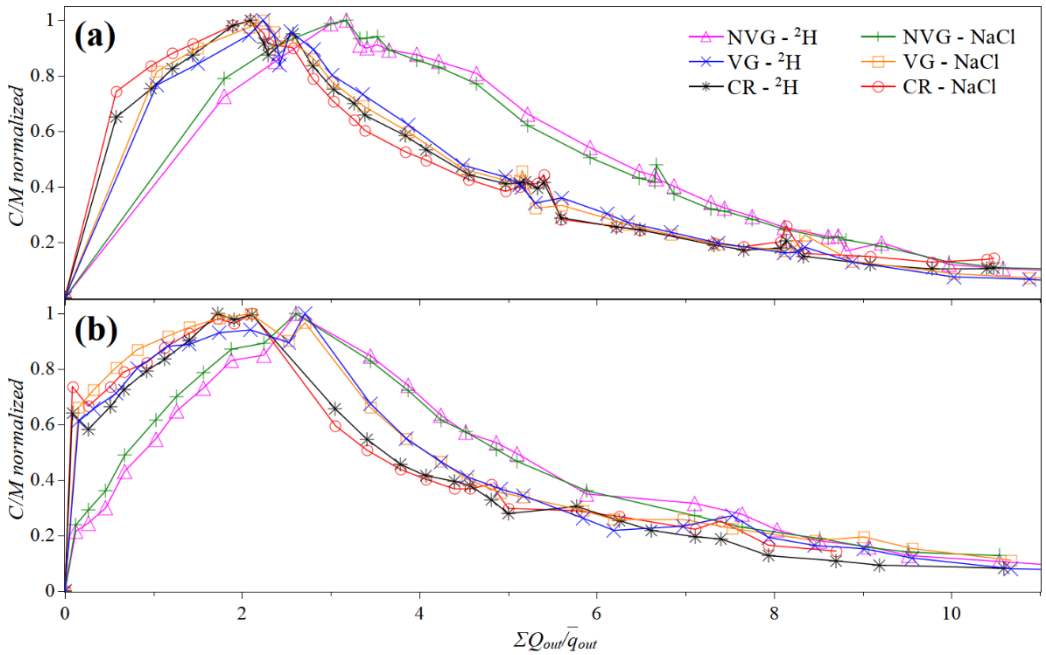

Figure 14. Normalized breakthrough curves of (a) 1st tracer test, (b) 2nd tracer test (all plots and tracer substances are plotted)

Flow interruptions resulted in small steps of the concentration curve (mainly control and vegetated testbed), which can be explained by enhanced diffusion during the flow interruption. However, diffusion is not a dominating transport process indicated by the negligible differences in the peak concentration and tailing between the two substances, and hence the diffusive exchange between different pore regions of a potentially present dual-porosity substrate is limited.

Despite differences in the sampling interval at the very beginning, a steeper increase in the tracer concentration can be observed in the control and vegetated boxes during the 2nd compared to the 1st tracer test. This could indicate preferential flowpaths along the living roots of the vegetated BioRoofs, though this could be induced by the different sampling interval or by different initial conditions of the substrate. More specifically, the initial water content of the substrate can affect the response of the system to the injected solutes; if the moisture is high prior to the tracer test, the concentration of the tracer in the first outflow will be low thus delaying the peak concentration relative to the cumulative outflow. Prior to the first tracer test, the substrate moisture was θ= 0.23 and θ= 0.21 for the control and vegetated testbeds, respectively, while prior to the second injection the substrate was slightly drier (θ=0.20 and θ=0.19). This might have resulted in

a quicker release of the solutes in the outflow during the second tracer test with drier initial conditions. Differences in the initial moisture between the vegetated and non-vegetated BioRoof might also explain the more gradual and slow increase of the tracer concentration in the outflow of the latter. In particular, prior to the second trace injection, the non-vegetated plot was 7% wetter than the vegetated and 6% wetter than the control. Therefore, it can be hypothesized that plants have triggered different initial conditions between the non-vegetated and vegetated plots due to the their influence on the water content of the substate, but it cannot be concluded that they have altered the hydraulic properties of the medium due to their rooting system.

The similarity between tracer curves from the 1st and 2nd experiment together with the lack of trend in the observed soil moisture suggests that the effect of bioclogging, if present, is negligible. According to Langergraber *et al.* (2009), vertical flow constructed wetlands do not experience clogging for organic load less than 20g COD m^{-2} d^{-1}. The same findings were reported in a similar study by Winter & Goetz (2003). In the current experiment, the organic load rate was approximately 1 to 1.5 gCOD m^{-2} d^{-1} with 3 resting days per week to favor oxidative degradation of the microbial biomass. As the literature suggests, a resting period of 3 days alleviates bioclogging by improving hydraulic conductivity and effective porosity of vertical flow contructed wetlands (Hua *et al.*, 2014). Zapater-Pereyra *et al.* (2016) reported that after injecting wastewater with approximately the same organic load rate as this study (1.2 gCOD m^{-2} d^{-1}) on a BioRoof for 551 days, no clogging occurred. However, this is highly dependent on the physical conditions and the biochemical processes that occur in the substrate and it is possible that a longer experimental campaign or a higher organic load would have resulted in the formation of a biofilm at the soil surface, due to the sorption of organic compounds on the soil matrix. Further findings are needed to validate this assumption and it is recommended that future experiments focus on longer experimental periods or higher organic load rates to clarify this behavior, which is crucial for the real world functioning of BioRoofs.

3.2 *Heat transport*

All three experimental plots reduced the differences between the daily maxima and minima temperatures (the diurnal temperature fluctuation). In general, higher thermal attenuation was achieved in Temperature Point 1 (TP1) compared to Temperature Point 2 (TP2) and in plots with vegetation (up to 25%) compared to the unvegetated (up to 20%). The average soil moisture was near the suggested value (θ_{avg}= 0.25) for optimal thermal gains of BioRoofs (Brunetti *et al.*, 2018).

Table 5. Measured temperature values in TP1, TP2 and average ambient temperature T (ºC)

Measurement Point		T_{min} (ºC)	T_{max} (ºC)	T_{avg} (ºC)	$T_{avg(6h)}$>25	
					Value (ºC)	Reduction
TP1	Vegetated	12.5	27.7	20.6	21.9	22%
	Non-Vegetated	13.2	29.5	22	23.9	14%
	Control	13.2	27.5	20.9	22.1	21%
TP2	Vegetated	12.8	27.7	20.7	21.9	22%
	Non-Vegetated	13.3	29	21.5	22.8	19%
	Control	13.2	28.5	21.1	22.5	20%
Ambient		9	36.4	21	28.1	-

Figure 15 shows the measured air (grey line) and the bottom temperatures (color lines) in the BioRoofs during the monitoring campaign. It is evident that all BioRoofs exhibit a significant thermal attenuation, with a maximum peak temperature reduction of 8.7 K on June 29th for the vegetated BioRoof. During that date the peak delay was approximately 6 hours. This thermal damping effect is visible during all the experiment and highlights the energetic benefits of the BioRoofs. For every six hours that the average ambient temperature was higher than 25 ºC (n=30, $T_{avg(6h)}$ = 28.1 ºC) the average bottom temperature of the testbeds was reduced by 6.2 K (-22%) in the vegetated testbed, thereby cutting the heat gains of a building. During those periods, the temperature peak was delayed by approximately 5 hours in all BioRoofs, with insignificant differences among the vegetated and non-vegetated testbeds. While the vegetated (green line in Figure 15) and the control (blue line in Figure 15) BioRoofs exhibit similar thermal behavior, the

non-vegetated (brown line in Figure 15) generally shows higher temperatures with lower peak reductions. In particular, the maximum reduction is 7.7 K (June 29th) and the thermal peaks ($T_{avg(6h)}$ > 25 ^{o}C) were on average moderated by 5.3 K (-19%). The differences between the vegetated and non-vegetated tesbeds suggest an appreciable role of the vegetation on the heat transport. This behavior is connected to the higher soil moisture observed in the non-vegetated BioRoof (Figure 11), which increases its thermal conductivity and capacity.

In all BioRoofs, the constant water feeding of the system, which increases the thermal conductivity of the substrate, seems to be counterbalanced by the evaporative cooling effect, as reported in Brunetti *et al.* (2018). However, at night the BioRoofs exhibited higher minima temperatures which can be beneficial during cold or mild nights, but could inhibit heat losses from buildings during warm nights. When the minimum night temperature exceeded 18 ^{o}C (n=5, $T_{avg(night)}$ = 18.6 ^{o}C), the bottom temperature of the BioRoofs was on average 2.3 K (13%) higher. The night temperature increase during warm nights ($T_{min(night)}$ > 18 ^{o}C) was generally less evident in the vegetated BioRoof (10%) compared to the average. Figure 16 shows the difference between the measured substrate (TP1) and gravel (TP2) temperature for the vegetated and non-vegetated BioRoofs, and provides an indication about the thermal fluxes during the experiment. The different behavior of the two testbeds is evident; the non-vegetated BioRoof is considerably more sensitive to the wastewater injection, as demonstrated by the multiple peaks in Figure 16. Due to the lack of vegetation cover, the soil surface is directly exposed to the chamber radiation and irrigation, which raises the soil surface moisture and reduces the surface albedo, thus increasing the incoming net radiation. This entering energy results in a higher soil temperature, which generates incoming heat fluxes (i.e., positive gradient). The heat travels across the BioRoof and accumulates in the drainage layer, thus inverting the heat flux at night (i.e., negative gradient). On the other hand, the vegetation layer damps the heat fluctuations in the BioRoof due to its shadowing effect, thus resulting in limited temperature gradients and in an overall more homogenous behavior of the system.

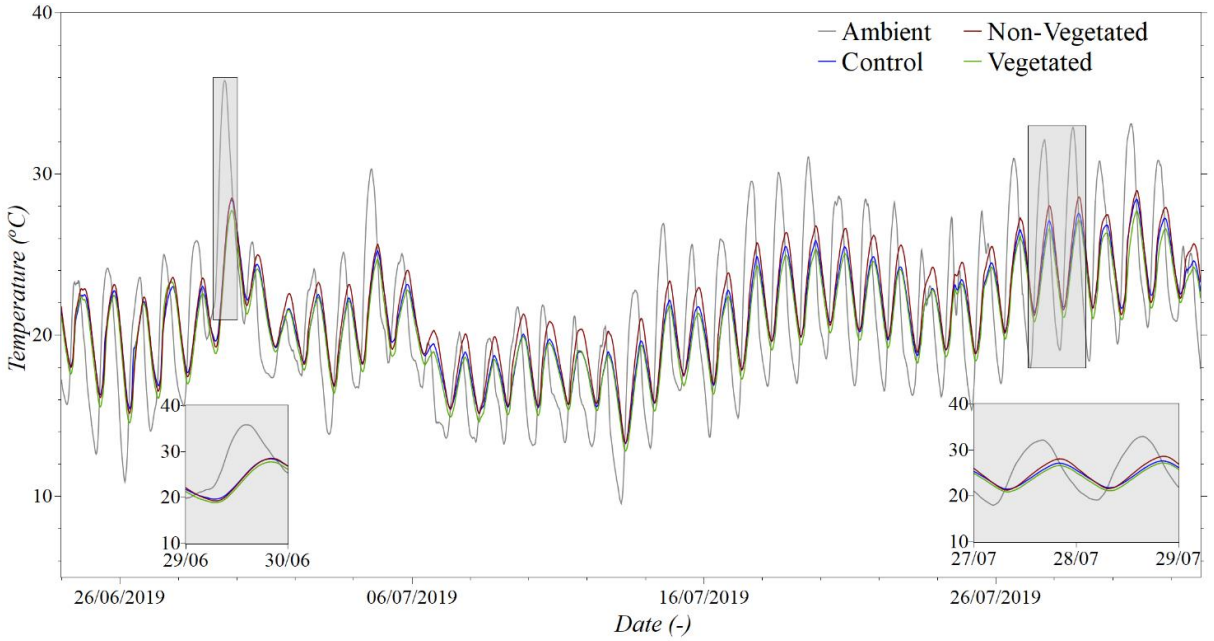

Figure 15. Measured ambient (grey line) and bottom temperature (TP2) of the three BioRoofs. The inset layers show the temperature during June 29th (bottom left corner) and July 28th and 29th (bottom right corner).

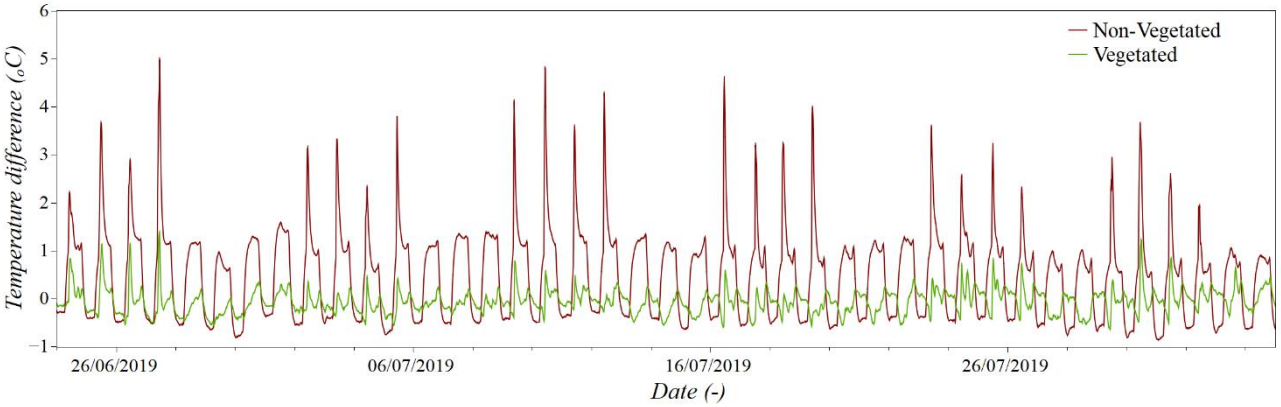

Figure 16. The difference between the measured substrate (TP1) and gravel (TP2) temperature for the vegetated (green line) and non-vegetated (brown line) BioRoofs. Positive and negative differences indicate incoming and outgoing heat fluxes, respectively

The temperature reduction and delay that the vegetated BioRoof achieved during the day can be used to avoid energy consumption peaks and shift the energy cooling demand during the warm nights, when the energy price is lower. Nevertheless, this is beyond the scope of the study and a cost-benefit assessment in the building scale is required to evaluate this finding.

3.3 *Reactive Nitrogen Transport*

The inorganic nitrogen species were analyzed in the inflow and outflow from the testbeds. The

concentration of Total Inorganic Nitrogen (TIN) in the influent and effluent is significantly different among the BioRoofs (Figure 17). Table 6 reports the mean, median and 90% confidence interval of the measured TIN from all three testbeds and the TIN in the injected wastewater and tap water. The control plot, which was irrigated with tap water, acted as a N source (3.7 mg L^{-1}) and agrees with what reported in previous studies dealing with green roof water quality analysis (Buffam et al., 2016; Vijayaraghavan et al., 2012). Figure 18 shows the nitrogen concentration of ammonium (NH_4^+), nitrite (NO_2^-) and nitrate (NO_3^-) in the outflow of the BioRoofs. The vast majority (approximately 98%) of TIN was in the form of $N\text{-}NO_3^-$, while the concentrations of $N\text{-}NO_2^-$ and $N\text{-}NH_4^+$ in the effluent reached a maximum of 0.35 mg L^{-1}. This difference can be easily identified from the y-axis of NO_3^- (Figure 18c) which is larger than NO_2^- and NH_4^+ by two orders of magnitude. Ammonium is known to be less mobile compared to nitrate and usually accumulates in the surface of topsoils, while the oxidation of nitrite to nitrate is almost instantaneous in the presence of nitrite oxidizers in the soil. On the contrary, the soluble nitrate is omnipresent in leachate of N-rich sources, such as municipal wastewater and organic substrates.

Table 6. Mean values and 90% confidence interval of Total Inorganic Nitrogen (TIN) concentration in the influent and effluent. (WW: wastewater, TW: tap water, RE: removal efficiency).

TIN	WW	Vegetated		Non-Vegetated		TW	Control
	mgN L^{-1}	mgN L^{-1}	RE	mgN L^{-1}	RE	mgN L^{-1}	mgN L^{-1}
5%	-	7.8	68%	18	25%	-	3.2
95%	-	10.1	58%	20.4	15%	-	4.3
Median	-	9	63%	19.6	18%	-	3.6
Mean	24	9.4	61%	19.5	19%	< 0.5	3.7

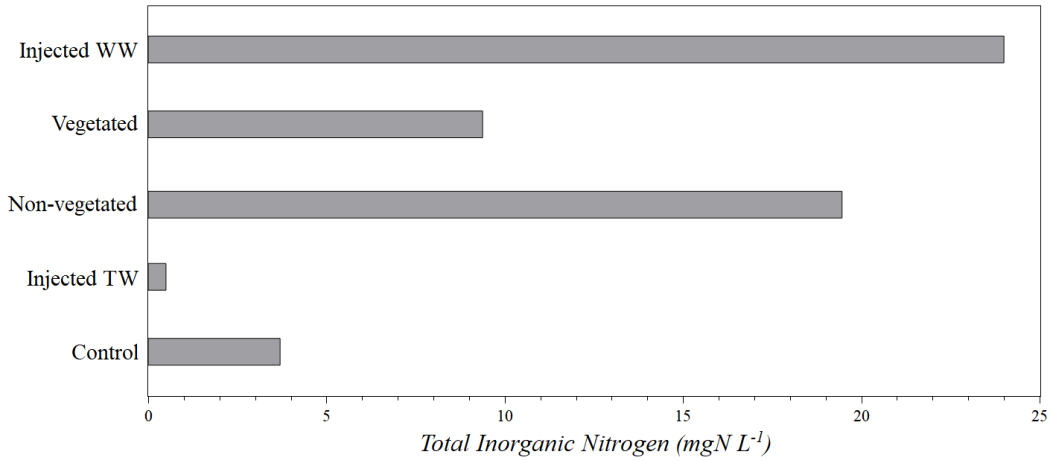

Figure 17. Measured Total Inorganic Nitrogen (TIN) in the influent and effluent of the testbeds. (WW: wastewater, TW: tap water)

Repeated laboratory measurements revealed that the Total Nitrogen (TN, as % of the mass) and Total Carbon (TC, as % of the mass) content in the BioRoof soil substrate range from 0.38% to 0.42% and from 3.8% to 4.4%, respectively. A relatively low C:N ratio (≈10) is generally associated with substantial soil nitrification processes, thus supporting the presence of nitrate in outflow of the control plot. Furthermore, the soil temperature (Figure 15) ranges between 12 and 27 °C, which is an optimal range for bacterial degradation (Sakai, 1959). In addition to that, the volumetric water content varies between 0.18 and 0.35, which corresponds to a pressure head ranging from approximately 10 to 1,000 cm. Ohte *et al.* (1997) demonstrated how moderately wet substrates favor nitrification processes, while dry and saturated conditions are limiting conditions. The highly aerobic characteristics of BioRoofs were reported also in Zapater-Pereyra *et al.* (2013, 2016). Altogether these factors creates an ideal environment for mineralisation and nitrification processes, which can explain the relatively high concentrations of nitrate in the CR effluent.

Despite the same amount of wastewater injected, the average nitrate concentration in the outflow of the non-vegetated BioRoof was 19.5 mg L^{-1} ($CI_{90\%}$=8.5 mg L^{-1}), which is significantly higher than that measured for the vegetated testbed (i.e., 9.4 mg L^{-1}, $CI_{90\%}$=7.5 mg L^{-1}). A two sample t-test was conducted between effluent concentrations from vegetated and non-vegetated BioRoofs assuming unequal variances, which revealed significant differences among the groups

with α=0.01, validating the contribution of plants in nitrogen attentuation. The vegetated BioRoof achieved a 61% reduction in the concentration of TIN, while the non-vegetated 19%. The optimal soil moisture conditions, induced by the irrigation pattern, avoids any root water stress, thus triggering a passive uptake of nitrate from the soil matrix into plants via transpiration streams. As a consequence, the nitrate concentration in the soil pore water are outflow are reduced. These results are in line with a review on shallow-bed constructed wetlands, reporting that plants had a positive effect on the removal efficiency of nitrogen (Vo *et al.*, 2019).

The linear fitting of the nitrate concentrations in the effluent suggests that there is an underlying opposite trend between the vegetated and non-vegetated BioRoofs, while this is less evident in the control which indicates a small reduction in the nitrate concetration over time (Figure 18). Although initially the concentration of nitrate was three times larger in the non-vegetated, it gradually decreases while the concentration of nitrate in the vegetated increases with time. The increase of the nitrate in VG suggests that plant uptake of nitrate decreased, resulting in a higher concentration of nitrate in the effluent. However, we cannot exclude the possibility of a delayed growth of the nitrifying bacterial population in the vegetated BioRoof, due to competion for ammonium with plants. According to Skiba *et al.* (2011) there is no general scientific consensus as to whether the plant roots, through assimilation of ammonium, are stronger competitors than the nitrifying bacterial population. On the other hand, the strongly aerobic conditions suggest that the predominant inorganic nitrogen form is nitrate (Xu *et al.*, 2012) and the increase of nitrates in the effluent can be accredited to a decrease in the plant uptake. It would be crucial to monitor the growth of the microbial biomass during the experimental campaign to understand the influence of plants on the trend of nitrates in the effluent of BioRoofs. Furthermore, a longer monitoring campaign is needed to investigate the long-term influence of plants on the removal efficiency of inorganic nitrogen.

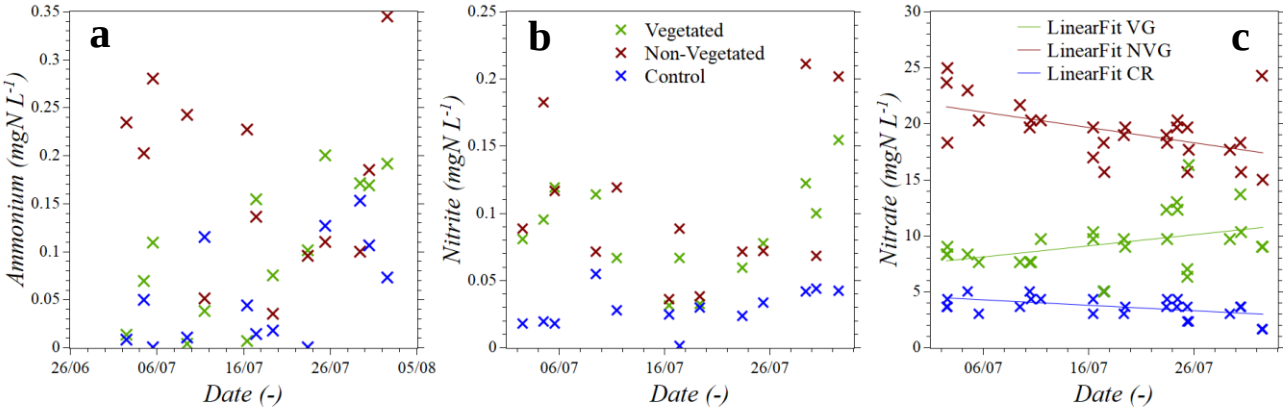

Figure 18. Measured ammonium (left), nitrites (middle), and nitrates (right) in the effluent from the BioRoofs (color marks)

3.4 *Summary of the results*

In general, the addition of the vegetation yielded positive effects by improving the hygrothermal performance of the BioRoof and provided a larger sink for nitrate, thus reducing the leaching from the system. It must be emphasized that during the last week, the dianthus plants experienced stress in both the vegetated and control BioRoofs, in contrast with the allysum that showed no sign of stress and continuously bloomed throughout the experiment (Figure 19). This suggests that plants did not experience any toxicity effect from the injection of wastewater.

The most important factor in the performance of the vegetated BioRoof was the volumetric water content that the irrigation pattern and the plants induced. Altough the cumulative hydrograph (Figure 12) suggests that the water retention of the non-vegetated BioRoof was sligthly higher, it is contradicted by the more precise measuments of the outflow and the soil moisture which demonstrate that the vegetated substrate, which was 4% drier due to plant transpiration, offered better water storage than the non-vegetated (Figure 11). Most of the water storage (39%) occurred during the first irrigation day, when the vegetated plot was up to 31% drier. The water-solute transport processes in the BioRoofs did not seem to be significantly different with the addition of the vegetation or the irrigation with wastewater and the difference in the release of the solutes relative to the cumulative outflow in the hydrographs can be attributed to the higher water content

of the non-vegetated testbed. The lower water content along with the leaf canopy substantially reduced and delayed all temperature peaks, especially during days that the air temperature reached 25 ^{o}C. Even more profound is the temperature difference inside the substrate, where the shading effect of the BioRoof provides big gains. The vegetated substrate is less susceptible to the environmental conditions (irrigation and air temperature), thus accumulating less heat during the night. The contribution of plants is also significant in reducing the concentration of nitrate from the water exiting the BioRoof, either by assimilating ammonium, which reduces the available N source for nitrifying bacteria, or by passively uptaking nitrate from the soil pore water due to the optimal moisture. The effluent can be utilised as a source of immediately available nitrogen for irrigation of gardens, roofs and parks or recycled in the building for non-potable uses, such as toilet flushing. In fact, the average concentration of the measured nitrate exiting the vegetated BioRoof was below the 11 mgN-NO_3^- L^{-1} drinking water limit suggested by WHO (2011) and U.S.EPA (2018). Further water quality assessments must indicate whether BioRoofs can provide purification as a stand-alone method or as an integral part of a more complex system by combining vertical flow and horizontal flow BioRoofs to achieve denitrification. Other studies suggest that due to their highly oxic conditions and reduced root water stress, vegetated BioRoofs offer great potential to treat specific wastewater compounds due to the phytoremediation capability of certain plant species (Vijayaraghavan, 2016). For instance, *Portulaca oleracea*, a widely distributed succulent plant, exhibited significant detoxification capabilities against phenolic endocrine disruptors (Imai *et al.*, 2007), and its use should in BioRoofs should be explored.

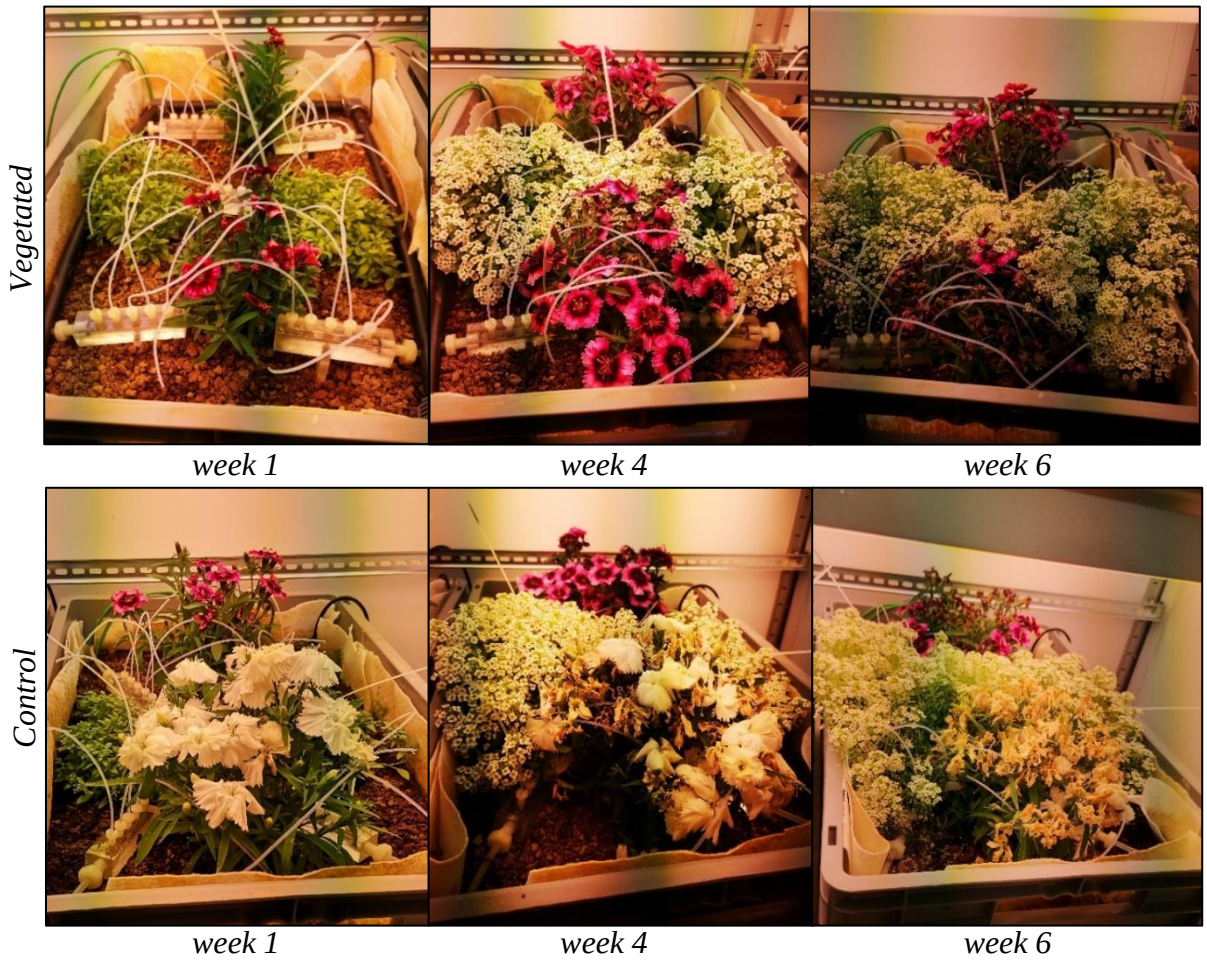

Figure 19. Planth growth during the monitoring campaign

4 CONCLUSIONS AND OUTLOOK

The main aim of the present study was to compare the environmental benefits of vegetated and non-vegetated BioRoofs in the Mediterrenean climate, as a novel sustainable decentralized solution in urban areas. For this purpose, we assessed the performance of three testbeds on their hydrology, thermal performance and inorganic nitrogen removal efficiency. A control testbed was irrigated with tap water to identify differences in the hydrological performance and the development of plants, due to the injection of wastewater. During 6-weeks of controlled irrigation, 96 liters of tap water were applied in the control plot and 192 liters of diluted domestic wastewater were injected in a vegetated and non-vegetated BioRoof combined. The results of the experimental campaign hereby presented and discussed led to significant conclusions and future directions, which can be summarized in few points:

- Both the vegetated and non-vegetated BioRoofs offer hydrological, thermal, and water quality benefits. In particular, the BioRoofs reduced the total water volume by over 30% and moderated high temperatures by 20%, while delaying the peaks by as much as 6 hours. Nitrification from the injected wastewater was achieved since the beginning of the experiment.
- The vegetation enhances the performance of the system in all aspects. In particular, the lower water content that plants induce, increases the available storage capacity of the BioRoof, thus reducing the outflow volume. Additionally, the drier soil and shadowing effect further reduces the temperature at the bottom of the BioRoof by 1 K, while minimizing the incoming net radiation in the substrate.
- The intermittent feeding of the system minimizes the plants water stress and favors the root water and solute uptake, thus reducing the concentration of reactive nitrogen by

61%. Despite that, the nitrate concentrations from the vegetated and non-vegetated BioRoofs followed opposite trends over time and could have converged if the experiment was continued.

- No bioclogging was observed from the tracer curves after 6 weeks of wastewater injection.
- The unsaturated operating conditions of BioRoofs and the reduced water stress can be exploited to maximize the oxic reactions in the porous media and the phytoremediation effect of the vegetation against specific compounds or contaminants of emerging concern.

Future studies should optimise BioRoof management practices by focusing on long-term campaigns and higher organic load rates to investigate: bioclogging of the BioRoof substrate, relatioship between removal efficiency of TIN and plants.

REFERENCES

Andrés-Doménech, I., Perales-Momparler, S., Morales-Torres, A. & Escuder-Bueno, I. (2018) 'Hydrological Performance of Green Roofs at Building and City Scales under Mediterranean Conditions', *Sustainability*, 10(9), p. 3105. doi: 10.3390/su10093105.

Ávila-Hernández, A., Simá, E., Xamán, J., Hernández-Pérez, I., Téllez-Velázquez, E. & Chagolla-Aranda, M. A. (2020) 'Test box experiment and simulations of a green-roof: Thermal and energy performance of a residential building standard for Mexico', *Energy and Buildings*, 209. doi: 10.1016/j.enbuild.2019.109709.

Balugani, E., Lubczynski, M. W., van der Tol, C. & Metselaar, K. (2018) 'Testing three approaches to estimate soil evaporation through a dry soil layer in a semi-arid area', *Journal of Hydrology*. doi: 10.1016/j.jhydrol.2018.10.018.

Becker, M. W. & Coplen, T. B. (2001) 'Use of deuterated water as a conservative artificial ground water tracer', *Hydrogeology Journal*. doi: 10.1007/s100400100157.

Berndtsson, R., Becker, P., Persson, A., Aspegren, H., Haghighatafshar, S., Jönsson, K., Larsson, R., Mobini, S., Mottaghi, M., Nilsson, J., Nordström, J., Pilesjö, P., Scholz, M., Sternudd, C., Sörensen, J. & Tussupova, K. (2019) 'Drivers of changing urban flood risk: A framework for action', *Journal of Environmental Management*. Elsevier, 240(March), pp. 47–56. doi: 10.1016/j.jenvman.2019.03.094.

Bevilacqua, P., Bruno, R. & Arcuri, N. (2020) 'Green roofs in a Mediterranean climate: energy performances based on in-situ experimental data', *Renewable Energy*. doi: 10.1016/j.renene.2020.01.085.

Brunetti, G., Porti, M. & Piro, P. (2018) 'Multi-level numerical and statistical analysis of the hygrothermal behavior of a non-vegetated green roof in a mediterranean climate', *Applied Energy*. Elsevier, 221(November 2017), pp. 204–219. doi: 10.1016/j.apenergy.2018.03.190.

Brunetti, G., Šimůnek, J. & Piro, P. (2016) 'A Comprehensive Analysis of the Variably Saturated Hydraulic Behavior of a Green Roof in a Mediterranean Climate', *Vadose Zone Journal*, 15(9), p. 0. doi: 10.2136/vzj2016.04.0032.

Brutsaert, W. (2014) 'Daily evaporation from drying soil: Universal parameterization with similarity', *Water Resources Research*. doi: 10.1002/2013WR014872.

Buffam, I., Mitchell, M. E. & Durtsche, R. D. (2016) 'Environmental drivers of seasonal variation in green roof runoff water quality', *Ecological Engineering*. doi: 10.1016/j.ecoleng.2016.02.044.

Buyantuyev, A. & Wu, J. (2010) 'Urban heat islands and landscape heterogeneity: linking spatiotemporal variations in surface temperatures to land-cover and socioeconomic patterns', *Landscape Ecology*, 25(1), pp. 17–33. doi: 10.1007/s10980-009-9402-4.

Carpenter, D. D. & Kaluvakolanu, P. (2011) 'Effect of Roof Surface Type on Storm-Water Runoff from Full-Scale Roofs in a Temperate Climate', *Journal of Irrigation and Drainage Engineering*, 137(3), pp. 161–169. doi: 10.1061/(ASCE)IR.1943-4774.0000185.

Cascone, S., Catania, F., Gagliano, A. & Sciuto, G. (2018) 'A comprehensive study on green roof performance for retrofitting existing buildings', *Building and Environment*. Elsevier, 136(February), pp. 227–239. doi: 10.1016/j.buildenv.2018.03.052.

Castiglia, R. & Wilkinson, S. J. (2019) 'Small-scale experiments of seasonal heat stress attenuation through a combination of green roof and green walls', *Journal of Cleaner Production*. Elsevier Ltd, (xxxx), p. 119443. doi: 10.1016/j.jclepro.2019.119443.

City of Toronto (2017) 'TORONTO MUNICIPAL CODE - CHAPTER 492, GREEN ROOFS'.

Dong, J., Lin, M., Zuo, J., Lin, T., Liu, J., Sun, C. & Luo, J. (2020) 'Quantitative study on the

cooling effect of green roofs in a high-density urban Area—A case study of Xiamen, China', *Journal of Cleaner Production*. Elsevier Ltd, 255, p. 120152. doi: 10.1016/j.jclepro.2020.120152.

European Commission (2013) 'COMMUNICATION FROM THE COMMISSION TO THE EUROPEAN PARLIAMENT, THE COUNCIL, THE EUROPEAN ECONOMIC AND SOCIAL COMMITTEE AND THE COMMITTEE OF THE REGIONS Green Infrastructure (GI) — Enhancing Europe's Natural Capital'.

European Environmental Agency (2018) *European waters Assessment of status and pressures 2018, Parents and Children Communicating with Society: Managing Relationships Outside of Home*. doi: 10.4324/9780203938607.

Feng, H. & Hewage, K. N. (2018) *Economic Benefits and Costs of Green Roofs, Nature Based Strategies for Urban and Building Sustainability*. Elsevier Inc. doi: 10.1016/B978-0-12-812150-4.00028-8.

Ferree, M. A. & Shannon, R. D. (2001) 'Evaluation of a second derivative UV/visible spectroscopy technique for nitrate and total nitrogen analysis of wastewater samples', *Water Research*, 35(1), pp. 327–332. doi: 10.1016/S0043-1354(00)00222-0.

FLL - Forschungsgesellschaft Landschaftsentwicklung Landschaftsbau (2008) 'The new Guideline for The Planning and Upkeep of Green-Roof Sites (Overview)', in *Federation of Green-Roof Associations, EFB, Conference Budapest 2008*.

FAO - Food and Agriculture Organisation of the United Nations (2016) 'Soil sealing', I6470EN/1/11.16.

Gagliano, A., Nocera, F., Detommaso, M. & Evola, G. (2016) 'Thermal behavior of an extensive green roof: Numerical simulations and experimental investigations', *International Journal of Heat and Technology*. doi: 10.18280/ijht.34S206.

GLA (2016) 'The London Plan: The Spatial Development Strategy For London Consolidated With Alterations Since 2011', *Greater London Authority*.

Hamburgische Investitions- und Förderbank - IFB Hamburg (2020) 'HAMBURGER GRÜNDACHFÖRDERUNG - Förderrichtlinie für die Herstellung von Dachbegrünung auf Gebäuden'.

Hill, M. J. (2010) 'Nitrates and nitrites from food and water in relation to human disease', in *Nitrates and Nitrites in Food and Water*. doi: 10.1533/9781855736559.163.

Holmes, D. E., Dang, Y. & Smith, J. A. (2019) *Nitrogen cycling during wastewater treatment*. 1st edn, *Advances in Applied Microbiology*. 1st edn. Elsevier Inc. doi: 10.1016/bs.aambs.2018.10.003.

Hua, G., Zeng, Y., Zhao, Z., Cheng, K. & Chen, G. (2014) 'Applying a resting operation to alleviate bioclogging in vertical flow constructed wetlands: An experimental lab evaluation', *Journal of Environmental Management*. doi: 10.1016/j.jenvman.2014.01.030.

Huang, C.-W., McDonald, R. I. & Seto, K. C. (2018) 'The importance of land governance for biodiversity conservation in an era of global urban expansion', *Landscape and Urban Planning*, 173, pp. 44–50. doi: 10.1016/j.landurbplan.2018.01.011.

Hutchinson, D., Abrams, P., Retzlaff, R. & Liptan, T. (2003) 'Stormwater monitoring two ecoroofs in Portland, Oregon, USA', *Greening Rooftops for Sustainable Communities*, pp. 1–18. Available at: http://www.portlandoregon.gov/bes/article/63098%5Cnhttp://www.portlandonline.com/shared/cfm/image.cfm?id=63098.

Imai, S., Shiraishi, A., Gamo, K., Watanabe, I., Okuhata, H., Miyasaka, H., Ikeda, K., Bamba, T. & Hirata, K. (2007) 'Removal of phenolic endocrine disruptors by Portulaca oleracea', *Journal of Bioscience and Bioengineering*. doi: 10.1263/jbb.103.420.

Imran, H. M., Kala, J., Ng, A. W. M. & Muthukumaran, S. (2018) 'Effectiveness of green and cool roofs in mitigating urban heat island effects during a heatwave event in the city of

Melbourne in southeast Australia', 197. doi: 10.1016/j.jclepro.2018.06.179.

Jafarinejad, S. (2020) 'A framework for the design of the future energy-efficient, cost-effective, reliable, resilient, and sustainable full-scale wastewater treatment plants', *Current Opinion in Environmental Science and Health*. doi: 10.1016/j.coesh.2020.01.001.

Kargas, G., Ntoulas, N. & Nektarios, P. A. (2013) 'Moisture content measurements of green roof substrates using two dielectric sensors', *HortTechnology*. doi: 10.21273/HORTTECH.23.2.177.

Langergraber, G., Leroch, K., Pressl, A., Sleytr, K., Rohrhofer, R. & Haberl, R. (2009) 'High-rate nitrogen removal in a two-stage subsurface vertical flow constructed wetland', *Desalination*, 246(1–3), pp. 55–68. doi: 10.1016/j.desal.2008.02.037.

Levermore, G., Parkinson, J., Lee, K., Laycock, P. & Lindley, S. (2017) 'Urban Climate The increasing trend of the urban heat island intensity', *Urban Climate*. Elsevier Inc., 24, pp. 360–368. doi: 10.1016/j.uclim.2017.02.004.

Liu, K. K. Y. & Minor, J. (2005) 'Performance Evaluation of an Extensive Green Roof', *Greening Rooftops for Sustainable Communities*. doi: 10.1109/ICEOE.2011.6013104.

Liu, W., Feng, Q., Chen, W., Wei, W., Si, J. & Xi, H. (2019) 'Runoff retention assessment for extensive green roofs and prioritization of structural factors at runoff plot scale using the Taguchi method', *Ecological Engineering*. Elsevier, 138(March), pp. 281–288. doi: 10.1016/j.ecoleng.2019.07.033.

Masi, F., Rizzo, A., Bresciani, R. & Conte, G. (2017) 'Constructed wetlands for combined sewer overflow treatment: Ecosystem services at Gorla Maggiore, Italy', *Ecological Engineering*. doi: 10.1016/j.ecoleng.2016.03.043.

Mohammad, A. G. & Adam, M. A. (2010) 'The impact of vegetative cover type on runoff and soil erosion under different land uses', *CATENA*, 81(2), pp. 97–103. doi: 10.1016/j.catena.2010.01.008.

Oberndorfer, E., Lundholm, J., Bass, B., Coffman, R. R., Doshi, H., Dunnett, N., Gaffin, S., Köhler, M., Liu, K. K. Y. & Rowe, B. (2007) 'Green Roofs as Urban Ecosystems: Ecological Structures, Functions, and Services', *BioScience*. doi: 10.1641/b571005.

Ohte, N., Tokuchi, N. & Suzuki, M. (1997) 'An in situ lysimeter experiment on soil moisture influence on inorganic nitrogen discharge from forest soil', *Journal of Hydrology*. doi: 10.1016/S0022-1694(96)03240-4.

Oke, T. R. (1982) 'The energetic basic of the urban heat island', *Quarterly Journal of the Royal Meteorological Society*, 108(455), pp. 1–24. doi: 10.1256/smsqj.45501.

Picarro (2014) 'δD and δ18O High-Precision Isotopic Water Analyzer'.

Rizvi, S. H., Alam, K. & Iqbal, M. J. (2019) 'Spatio -temporal variations in urban heat island and its interaction with heat wave', *Journal of Atmospheric and Solar-Terrestrial Physics*. Elsevier Ltd, 185(February), pp. 50–57. doi: 10.1016/j.jastp.2019.02.001.

Rosenzweig, C., Solecki, W. D., Parshall, L., Lynn, B., Cox, J., Goldberg, R., Hodges, S., Gaffin, S., Slosberg, R. B., Savio, P., Dunstan, F. & Watson, M. (2009) 'Mitigating new york city's heat island integrating stakeholder perspectives and scientific evaluation', *Bulletin of the American Meteorological Society*. doi: 10.1175/2009BAMS2308.1.

Sakai, H. (1959) 'Effect of temperature on nitrification in soils', *Soil Science and Plant Nutrition*. Taylor & Francis Group , 4(4), pp. 159–162. doi: 10.1080/00380768.1959.10430879.

Sanchez, L. & Reames, T. G. (2019) 'Urban Forestry & Urban Greening Cooling Detroit : A socio-spatial analysis of equity in green roofs as an urban heat island mitigation strategy', *Urban Forestry & Urban Greening*. Elsevier, 44(July 2018), p. 126331. doi: 10.1016/j.ufug.2019.04.014.

Sandoval, V., Suárez, F., Vera, S., Pinto, C., Victorero, F., Bonilla, C., Gironás, J., Bustamante, W., Rojas, V. & Pastén, P. (2015) 'Impact of the properties of a green roof substrate on its hydraulic and thermal behavior', *Energy Procedia*. Elsevier B.V., 78, pp. 1177–1182. doi:

10.1016/j.egypro.2015.11.097.
Seyfried, M. S., Grant, L. E., Du, E. & Humes, K. (2005) 'Dielectric loss and calibration of the hydra probe soil water sensor', *Vadose Zone Journal*, 4(4), pp. 1070–1079. doi: 10.2136/vzj2004.0148.
Sims, A. W., Robinson, C. E., Smart, C. C. & O'Carroll, D. M. (2019) 'Mechanisms controlling green roof peak flow rate attenuation', *Journal of Hydrology*. Elsevier, 577(July), p. 123972. doi: 10.1016/j.jhydrol.2019.123972.
Sims, A. W., Robinson, C. E., Smart, C. C., Voogt, J. A., Hay, G. J., Lundholm, J. T., Powers, B. & Carroll, D. M. O. (2016) 'Retention performance of green roofs in three different climate regions', *Journal of Hydrology*. Elsevier B.V., 542, pp. 115–124. doi: 10.1016/j.jhydrol.2016.08.055.
Skiba, M. W., George, T. S., Baggs, E. M. & Daniell, T. J. (2011) 'Plant influence on nitrification', in *Biochemical Society Transactions*. doi: 10.1042/BST0390275.
Song, U., Kim, E., Bang, J. H., Son, D. J., Waldman, B. & Lee, E. J. (2013) 'Wetlands are an effective green roof system', *Building and Environment*. Elsevier Ltd, 66, pp. 141–147. doi: 10.1016/j.buildenv.2013.04.024.
Susca, T. (2019) 'Green roofs to reduce building energy use? A review on key structural factors of green roofs and their effects on urban climate', *Building and Environment*. Elsevier, 162(June), p. 106273. doi: 10.1016/j.buildenv.2019.106273.
U.S. Environmental Protection Agency (2008) 'Urban Heat Island Basics. In Reducing Urban Heat Island: Compendium of Strategies'.
U.S. Environmental Protection Agency (2014) 'Energy Efficiency in Water and Wastewater Facilities', *U.S. Environmental Protection Agency*.
U.S. Environmental Protection Agency (2018) '2018 Edition of the Drinking Water Standards and Health Advisories', *United States Environmental Protection Agency*, (March), pp. 2–6. doi: EPA 822-S-12-001.
United Nations (2018) *World Urbanization Prospects*, *Demographic Research*. doi: 10.4054/demres.2005.12.9.
Van, P. T. H., Tin, N. T., Hien, V. T. D., Quan, T. M., Thanh, B. X., Hang, V. T., Tuc, D. Q., Dan, N. P., Khoa, L. Van, Phu, V. Le, Son, N. T., Luong, N. D., Kwon, E., Park, C., Jung, J., Yoon, I. & Lee, S. (2015) 'Nutrient removal by different plants in wetland roof systems treating domestic wastewater', *Desalination and Water Treatment*. doi: 10.1080/19443994.2014.915767.
VanWoert, N., Rowe, D. B. & Rugh, C. (2003) 'Green roof slope, substrate depth, and vegetation influence runoff', *Hortscience*.
Vijayaraghavan, K. (2016) 'Green roofs: A critical review on the role of components, benefits, limitations and trends', *Renewable and Sustainable Energy Reviews*. doi: 10.1016/j.rser.2015.12.119.
Vijayaraghavan, K., Joshi, U. M. & Balasubramanian, R. (2012) 'A field study to evaluate runoff quality from green roofs', *Water Research*. doi: 10.1016/j.watres.2011.12.050.
Vo, T.-D.-H., Bui, X.-T., Lin, C., Nguyen, V.-T., Hoang, T.-K.-D., Nguyen, H.-H., Nguyen, P.-D., Ngo, H. H. & Guo, W. (2019) 'A mini-review on shallow-bed constructed wetlands: A promising innovative green roof', *Current Opinion in Environmental Science & Health*. Elsevier Ltd, 12, pp. 38–47. doi: 10.1016/j.coesh.2019.09.004.
Vo, T. D. H., Bui, X. T., Nguyen, D. D., Nguyen, V. T., Ngo, H. H., Guo, W., Nguyen, P. D., Nguyen, C. N. & Lin, C. (2018) 'Wastewater treatment and biomass growth of eight plants for shallow bed wetland roofs', *Bioresource Technology*. doi: 10.1016/j.biortech.2017.09.194.
Vo, T. D. H., Do, T. B. N., Bui, X. T., Nguyen, V. T., Nguyen, D. D., Sthiannopkao, S. & Lin, C. (2017) 'Improvement of septic tank effluent and green coverage by shallow bed wetland

roof system', *International Biodeterioration and Biodegradation*. doi: 10.1016/j.ibiod.2017.05.012.

Vymazal, J. (2018) 'Constructed wetlands for wastewater treatment', *Encyclopedia of Ecology*, 1(April 2018), pp. 14–21. doi: 10.1016/B978-0-12-409548-9.11238-2.

Winter, K. J. & Goetz, D. (2003) 'The impact of sewage composition on the soil clogging phenomena of vertical flow constructued wetlands', in *Water Science and Technology*. doi: 10.2166/wst.2003.0268.

World Health Organization (2011) 'Nitrate and Nitrite in Drinking Water'. doi: 10.17226/9038.

Xu, G., Fan, X. & Miller, A. J. (2012) 'Plant Nitrogen Assimilation and Use Efficiency', *Annual Review of Plant Biology*. doi: 10.1146/annurev-arplant-042811-105532.

Yamashita, T. & Yamamoto-Ikemoto, R. (2014) 'Nitrogen and Phosphorus Removal from Wastewater Treatment Plant Effluent via Bacterial Sulfate Reduction in an Anoxic Bioreactor Packed with Wood and Iron', *International Journal of Environmental Research and Public Health*, 11(9), pp. 9835–9853. doi: 10.3390/ijerph110909835.

Zapater-Pereyra, M., Van Dien, F., Van Bruggen, J. J. A. & Lens, P. N. L. (2013) 'Material selection for a constructed wetroof receiving pre-treated high strength domestic wastewater', *Water Science and Technology*, 68(10), pp. 2264–2270. doi: 10.2166/wst.2013.483.

Zapater-Pereyra, M., Lavrnić, S., van Dien, F., van Bruggen, J. J. A. & Lens, P. N. L. (2016) 'Constructed wetroofs: A novel approach for the treatment and reuse of domestic wastewater', *Ecological Engineering*, 94, pp. 545–554. doi: 10.1016/j.ecoleng.2016.05.052.

Ziogou, I., Michopoulos, A., Voulgari, V. & Zachariadis, T. (2017) 'Energy, environmental and economic assessment of electricity savings from the operation of green roofs in urban office buildings of a warm Mediterranean region', *Journal of Cleaner Production*. Elsevier Ltd, 168, pp. 346–356. doi: 10.1016/j.jclepro.2017.08.217.

City of Toronto (2017) 'TORONTO MUNICIPAL CODE - CHAPTER 492, GREEN ROOFS'. Available at: https://www.toronto.ca/legdocs/municode/1184_492.pdf

Food and Agriculture Organisation of the United Nations (2016) 'Soil sealing', I6470EN/1/11.16. Available at: http://www.fao.org/3/a-i6470e.pdf

Hamburgische Investitions- und Förderbank - IFB Hamburg (2020) 'HAMBURGER GRÜNDACHFÖRDERUNG - Förderrichtlinie für die Herstellung von Dachbegrünung auf Gebäuden'. Available at: https://www.ifbhh.de/api/services/document/696

Affidavits

I hereby declare that I am the sole author of this work; no assistance other than that permitted has been used and all quotes and concepts taken from unpublished sources, published literature or the internet in wording or in basic content have been identified by footnotes or with precise source citations.